SOCIETY FOR EXPERIMENTAL BIOLOGY

Journal of Experimental Botany, Vol. 72, No. 18 pp. 6544–6569, 2021
https://doi.org/10.1093/jxb/erab258 Advance Access Publication 9 June 2021
This paper is available online free of all access charges (see https://academic.oup.com/jxb/pages/openaccess for further details)

RESEARCH PAPER

Transcriptional, hormonal, and metabolic changes in susceptible grape berries under powdery mildew infection

Diana Pimentel[1], Rute Amaro[1,*], Alexander Erban[2,*], Nuria Mauri[3,*], Flávio Soares[1], Cecília Rego[4], José M. Martínez-Zapater[3], Axel Mithöfer[5], Joachim Kopka[2] and Ana Margarida Fortes[1,†]

[1] BioISI – Biosystems and Integrative Sciences Institute, Faculty of Sciences, University of Lisbon, Campo Grande, 1749-016 Lisboa, Portugal
[2] Max-Planck-Institut für Molekulare Pflanzenphysiologie, 14476 Potsdam-Golm, Germany
[3] Instituto de Ciencias de la Vid y del Vino, CSIC-UR-Gobierno de La Rioja, Ctra. de Burgos km 6, 26007 Logroño, Spain
[4] Instituto Superior de Agronomia, Universidade de Lisboa, Tapada da Ajuda, 1349-017 Lisboa, Portugal
[5] Research Group Plant Defense Physiology, Max-Planck-Institute for Chemical Ecology, 07745 Jena, Germany

* These authors contributed equally to this work.
† Correspondence: amfortes@fc.ul.pt

Received 19 November 2020; Editorial decision 1 June 2021; Accepted 8 June 2021

Editor: Ariel Vicente, CONICET – National University of La Plata, Argentina

Abstract

Grapevine (*Vitis vinifera*) berries are extremely sensitive to infection by the biotrophic pathogen *Erysiphe necator*, causing powdery mildew disease with deleterious effects on grape and wine quality. The combined analysis of the transcriptome and metabolome associated with this common fungal infection has not been previously carried out in any fruit. In order to identify the molecular, hormonal, and metabolic mechanisms associated with infection, healthy and naturally infected *V. vinifera* cv. Carignan berries were collected at two developmental stages: late green (EL33) and early véraison (EL35). RNA sequencing combined with GC–electron impact ionization time-of-flight MS, GC–electron impact ionization/quadrupole MS, and LC–tandem MS analyses revealed that powdery mildew-susceptible grape berries were able to activate defensive mechanisms with the involvement of salicylic acid and jasmonates and to accumulate defense-associated metabolites (e.g. phenylpropanoids, fatty acids). The defensive strategies also indicated organ-specific responses, namely the activation of fatty acid biosynthesis. However, defense responses were not enough to restrict fungal growth. The fungal metabolic program during infection involves secretion of effectors related to effector-triggered susceptibility, carbohydrate-active enzymes and activation of sugar, fatty acid, and nitrogen uptake, and could be under epigenetic regulation. This study also identified potential metabolic biomarkers such as gallic, eicosanoic, and docosanoic acids and resveratrol, which can be used to monitor early stages of infection.

Keywords: Biotic stress, *Erysiphe necator*, grapevine, hormonal profiling, metabolome, plant defense, powdery mildew, transcriptome, susceptibility, *Vitis vinifera*.

Abbreviations: CAZymes, carbohydrate-active enzymes; EL33, late green stage; EL35, early véraison stage; ETI, effector-triggered immunity; PAMP, pathogen-associated molecular pattern; PM, powdery mildew; PRR, pattern-recognition receptor; PTI, PAMP-triggered immunity.

Introduction

Grapevine (*Vitis vinifera* L.) is a perennial woody plant highly susceptible to several abiotic and biotic stresses. Powdery mildew (PM) is one of the most dramatic diseases affecting grape production worldwide. It is caused by the ascomycete fungus *Erysiphe necator* Schw. (syn. *Uncinula necator* [Schw.] Burr.), an obligate biotrophic fungus that infects berry clusters and predisposes them to bunch rot infections (Calonnec *et al.*, 2004; Gadoury *et al.*, 2007, 2012). Eurasia-originated *V. vinifera* species are more susceptible to PM than the native North American *Vitis* species (Qiu *et al.*, 2015). Moreover, resistance to PM was also found in Chinese accessions of non-*vinifera* species, namely *V. romanetti* (Riaz *et al.*, 2011), *V. pseudoreticulata* (Wang *et al.*, 1995; Weng *et al.*, 2014) and *V. piasezkii* (Pap *et al.*, 2016), as well as in Central Asian accessions of *V. vinifera* (Hoffmann *et al.*, 2008; Amrine *et al.*, 2015). Since most of the cultivars used for wine and table grape production belong to *V. vinifera*, PM has spread to all vinicultural regions, and the control strategy is entirely dependent on the widespread application of sulfur-based and synthetic fungicides resulting in environmental poisoning and an impact on health.

During infection, the *E. necator* conidia form the appressorium that ruptures the cell wall and penetrates the plant cell, and then a feeding structure (haustorium) responsible for the dynamic exchanges between the fungus and the host cells is formed (Gadoury *et al.*, 2012). Several defense mechanisms to prevent pathogen penetration and colonization have been described in plants (Jones and Dangl, 2006). The two primary defense responses are pathogen-associated molecular pattern (PAMP)-triggered immunity (PTI) and effector-triggered immunity (ETI). Both responses take place consecutively and are interconnected. PM species adapted to a specific host are thought to release effectors to repress PTI, resulting in effector-triggered susceptibility. In response, host plants have evolved ETI as a second layer of resistance whereby these PTI-suppressing effector molecules are detected by resistance (*R*) genes that, in turn, activate several defense responses, including programmed cell death (Gadoury *et al.*, 2012). Most characterized plant *R*-genes encode proteins with leucine-rich repeat domains (LRRs), a central nucleotide-binding site (NB), and a variable N terminus (Jones and Dangl, 2006). Several genes involved in PM resistance have been identified in *Vitaceae* species such as those coding for pathogenesis-related (PR) proteins and stilbene synthases, and those involved in defense signal perception and transduction (reviewed by Qiu *et al.*, 2015).

Plant hormones are also essential in biotic stress responses, including salicylic acid (SA), jasmonic acid (JA), and ethylene. SA is classically related to response against biotrophic and hemibiotrophic pathogens, whereas JA and ethylene are central players in resistance to necrotrophic pathogens (Glazebrook, 2005). The basal levels of SA were shown to be higher in resistant *V. aestivalis* cv. Norton than in susceptible *V. vinifera* cv. Cabernet Sauvignon (Fung *et al.*, 2008). On the other hand, induction of JA and ethylene signaling has been associated with the elicitation of resistance and associated defense responses against powdery mildew in grapevine (Belhadj *et al.*, 2006, 2008).

Most of the studies on responses to fungal infections have focused on grapevine leaves, and little is known about the defense mechanisms in fruits. The actual effect of powdery mildew in grape berry and wine quality is controversial since sugar content of infected berries and resulting wines was reported to be both increased (Ough and Berg, 1979; Calonnec *et al.*, 2004) and decreased (Gadoury *et al.*, 2001), as well as their anthocyanin content being both increased and decreased (Ough and Berg, 1979; Piermattei *et al.*, 1999; Calonnec *et al.*, 2004).

Erysiphe necator affects mainly green tissues and, during normal ripening, grape berries develop an ontogenetic, i.e. age-related, resistance (Gadoury *et al.*, 2003; Ficke *et al.*, 2003). The period of fruit susceptibility is in general small, and resistance to PM in several *V. vinifera* cultivars increases around 2–4 weeks after bloom (Gadoury *et al.*, 2003; Ficke *et al.*, 2003). This is characterized by a reduction of penetration rate, near-immunity to new infections or to colonization of established colonies, and changes in latent period and sporophore density (Ficke *et al.*, 2003). Nevertheless, Gadoury *et al.* (2007) observed that berries could still support inconspicuous colonies after the onset of ontogenetic resistance, and this was associated with the presence of epiphytic microorganisms, *Botrytis cinerea*, and insects, that are attracted by specific volatiles.

Mechanisms behind grapevine resistance or susceptibility are highly complex, and despite the various studies performed so far, PM defense responses remain unclear, particularly in infected fruits. Therefore, in this study, we applied high throughput technologies combined with targeted approaches to shed light on how extremely susceptible grape berries (*V. vinifera* cv. Carignan) respond to natural PM infection at the early stages of ripening. The data suggests the activation of defensive mechanisms in response to PM infection, as previously observed in leaves (Fung *et al.*, 2008). However, certain responses seem to be differently modulated in berries and leaves, suggesting organ-specific mechanisms. Furthermore, our results provide novel insights concerning the hormonal regulation of defense against *E. necator* with the putative involvement of jasmonates, often associated with response against necrotrophs (Coelho *et al.*, 2019).

Materials and methods

Sampling

Grape berry clusters (*V. vinifera* L. cv. Carignan) were collected in 2017 from a commercial vineyard subjected to regular phytosanitary treatments at Torres Vedras region, Portugal (39°04′43.2″N, 9°20′58.9″W). Sampling was performed in two conditions, healthy berries and naturally infected berries, at two developmental stages, late green (EL33) and early véraison (EL35; 25–30% colored berries). For each condition (PM infected and control) and

time point, four to five biological replicates (corresponding to four to five clusters from different plants, 20–25 berries from each cluster) were collected on 13 July and 2 August 2017 after visual inspection of symptoms. Grape clusters were harvested around 11.30 h and immediately frozen in liquid nitrogen, transported in dry ice to the laboratory, and stored at −80 °C until further use. Prior to transcriptomic and metabolomic analysis, berries were deseeded and ground. Three to four replicates were used for metabolomics and hormone quantification and some of those samples were pooled to obtain three independent biological replicates for RNA-seq analysis.

DNA extraction and biomass quantification

DNA was extracted according to Lodhi *et al.* (1994) with some modifications. Before the RNase A purification, a treatment with 1/10 vol 2 M potassium acetate (1 h on ice) was added to the protocol to precipitate polysaccharides. Fungal biomass accumulation was measured relatively by real-time PCR (qPCR), according to Jones *et al.* (2014), by amplifying the *E. necator* elongation factor (*EnEF1*, KHJ34692) and the grapevine actin (*VvActin*) as reference (Supplementary Table S1).

RNA extraction

RNA extraction was performed as described by Coelho *et al.* (2019). A DNase treatment was carried out using TURBO DNase according to the supplier's instructions (Thermo Fisher Scientific, USA). RNA was then purified using Spectrum Plant Total RNA kit (Sigma-Aldrich, USA).

RNA-seq and differential gene expression analysis

RNA-seq was performed at the Centre for Genomic Regulation (CRG, Barcelona, Spain). The cDNA libraries were prepared using the TruSeq Stranded mRNA Sample Prep kit v2 (Illumina, ref. RS-122-2101/2) using 600 ng of total RNA according to the manufacturer's protocol. Poly(A)-mRNA selection using streptavidin-coated magnetic beads and subsequent RNA fragmentation to 300 bp was performed. Final libraries were analysed using Agilent DNA 1000 chip to check the quality. Library sequencing was performed on an Illumina HiSeq2500 sequencer using V4 chemistry (Illumina) and ~50 million paired-end strand-specific reads of 75 bp were produced per sample.

Reads alignment to the concatenated PN40024 12X.0 grapevine reference genome assembly (Jaillon *et al.*, 2007) and *E. necator* C-strain scaffolds (Jones *et al.*, 2014) was performed using HISAT2 version 2.1.0 with two consecutive mapping steps in order to find the splice sites independently of the annotations (Kim *et al.*, 2015). Potential PCR duplicates were removed with rmdup of SAMtools (http://samtools.sourceforge.net/, v. 1.3.1). After filtering, only the uniquely mapped reads with concordant insert size and orientation were used for further analysis. The htseq-count tool (version0.11.1) of HTSeq (Anders *et al.*, 2015) was used for strand-specific counting of read-pairs mapped to the exon regions annotated in the grapevine 12X V1 and *E. necator* genomes (Supplementary Table S2). Counts per gene were summarized and the dataset was balanced following the trimmed mean of M-values (TMM) method (Robinson and Oshlack, 2010) implemented in edgeR version 3.24.3 (Robinson *et al.*, 2010). Depth and gene length were normalized transforming pair-read to fragments per kb per million counts (FPKM) with rpkm function (genes were considered as expressed with mean FPKM in three replicates >1). After dispersion between samples was evaluated, an ANOVA-like test was run for any pairwise comparison with the exactTest function. Obtained *P*-values were re-adjusted (by the Benjamini–Hochberg procedure) and the significant genes were filtered out by false discovery rate (FDR) of ≤0.05 and fold change of ≥2.0 or ≤–2.0.

Functional analysis of differentially expressed genes

The list of differentially expressed genes (DEGs) was analysed using FatiGO (Al-Shahrour *et al.*, 2007) to identify functional categories significantly enriched according to the classification of 12X V1 annotation (Grimplet *et al.*, 2012). FatiGO uses Fisher's exact test to compare each DEG list with the list of total non-redundant transcripts housed in the grapevine 12X V1 gene predictions (Grimplet *et al.*, 2012); significantly enriched categories were selected considering the corrected *P*-value ≤0.05 (Benjamini–Hochberg correction for multiple testing).

Real-time PCR

First-strand cDNA was synthesized from 2 µg of total RNA, according to Fortes *et al.* (2011). Real-time PCRs (qPCRs) were carried out using the StepOne Real-Time PCR System (Thermo Fisher Scientific, USA). Cycling conditions were 95 °C for 10 min, followed by 42 cycles of 95 °C for 15 s and primers' annealing temperature for 1 min. Relative expression data were obtained from three to four biological replicates and duplicate technical replicates (in separate plates). The standard curve was built using a serial dilution of mixtures of all cDNAs analysed (1:1, 1:4, 1:16, 1:64, and 1:256), and used to check primer efficiency. Data were normalized using the expression curves of the actin gene (VIT_04s0044g00580) and elongation factor 1α gene (VIT_06s0004g03220). All primers used are shown in Supplementary Table S1.

Soluble metabolites

The profiling of soluble metabolites was performed by gas chromatography coupled to electron impact ionization time-of-flight mass spectrometry (GC-EI/TOF-MS), as specified by Dethloff *et al.* (2014). Soluble metabolites were extracted, as previously described by Agudelo-Romero *et al.* (2013), from 300±30 mg (fresh weight) of deep-frozen powder by 1 ml ethylacetate for 2 h of agitation at 30 °C. Extracts were centrifuged for 5 min at 18 000 *g*, and two aliquots of 300 µl from the ethylacetate fraction were dried by vacuum concentration and stored at −20 °C.

Chemical derivatization and retention index calibration were performed prior to injection, as described by Dethloff *et al.* (2014). GC-EI/TOF-MS analysis was performed using an Agilent 6890N24 gas chromatograph (Agilent Technologies, Germany) connected to a Pegasus III time-of-flight mass spectrometer (LECO Instrumente GmbH, Germany), with splitless injection onto a Varian FactorFour capillary column (VF-5 ms) of 30 m length, 0.25 mm inner diameter, and 0.25 mm film thickness (Varian-Agilent Technologies, Germany). Chromatograms were acquired, visually controlled, baseline corrected, and exported in NetCDF file format using ChromaTOF software (Version 4.22; LECO, St Joseph, MI, USA).

Compounds were identified by mass spectra and retention time index matching to the Golm Metabolome Database (Kopka *et al.*, 2005; Hummel *et al.*, 2010) using TagFinder software (Luedemann *et al.*, 2008). Guidelines for manually supervised metabolite identification were the presence of at least three specific mass fragments per compound and a retention index deviation of less than 1.0 % (Strehmel *et al.*, 2008). Metabolite intensities were normalized by sample fresh weight and internal standard (C_{22}) and maximum scaled, i.e. the maximum scaled normalized response. Log_2-transformed response ratios were calculated to approximate normal distribution for statistical analysis.

Volatile metabolites

Volatile profiling used 500±50 mg (fresh weight) of deep-frozen grape berry powder and was performed by solid-phase microextraction (SPME) and GC coupled to an EI/quadrupole MS (GC-EI/QUAD-MS) using an Agilent 5975B VL GC-MSD system and a StableFlex SPME-fiber with 65 µm polydimethylsiloxane/divinylbenzene (PDMS-DVB) coating (Supelco, USA) as described by Vallarino *et al.* (2018). SPME samples were taken from the headspace with 10 min incubation at 45 °C, 5 min adsorption at 45 °C,

and 1 min desorption at 250 °C and transferred onto a DB-624 capillary column with 60 m length, 0.25 mm inner diameter, and 1.40 µm film thickness (Agilent Technologies, Germany). GC temperature programming was 2 min isothermal at 40°C followed by a 10 °C/min ramp to 260 °C final temperature, which was held constant for 10 min. The Agilent 5975B VL GC-MSD system was operated with a constant flow of helium at 1.0 ml/min. Desorption from the SPME fiber was at 16.6 psi with an initial 0.1 min pulsed-pressure at 25 psi. The subsequent purge was 1 min at a purge flow of 12.4 ml/min. System stability was controlled and the sample sequence randomized. GC-EI/QUAD-MS chromatograms were acquired with mass range set to 30–300 m/z and a 20 Hz scan rate. Chromatograms were acquired, visually controlled, and exported in NetCDF file format using Agilent ChemStation software (Agilent) and baseline-corrected with ChromaTOF software (Version 4.22; LECO).

Compounds were identified using TagFinder software (Luedemann *et al.*, 2008) and the reference collection of the Golm Metabolome Database for volatile compounds (Kopka *et al.*, 2005; Hummel *et al.*, 2010). Guidelines for manually supervised identification were the presence of at least three specific mass fragments per compound and a retention time deviation of less than 3%. Metabolite intensities were normalized by sample fresh weight and maximum scaled, i.e. the maximum scaled normalized response. Log_2-transformed response ratios were calculated to approximate normal distribution for statistical analysis.

Hormonal profiling

About 30 mg of berry samples previously freeze-dried at −40 °C for 3 d were extracted in 1.5 ml methanol containing 60 ng D_4-SA (Santa Cruz Biotechnology, USA), 60 ng D_6-JA (HPC Standards GmbH, Germany), 60 ng D_6-abscicis acid (ABA) (Santa Cruz Biotechnology), and 12 ng D_6-jasmonoyl isoleucine (JA-Ile) (HPC Standards GmbH) as internal standards. Samples were agitated at room temperature for 10 min. The homogenate was mixed for 30 min and centrifuged at 15 000 *g* for 20 min at 4 °C and the supernatant was collected. The homogenate was re-extracted with 500 µl methanol, centrifuged, and supernatants were pooled. The combined extracts were evaporated under reduced pressure at 30 °C and dissolved in 500 µl methanol.

Phytohormone analysis was performed by LC–tandem mass spectrometry (MS/MS) as in Heyer *et al.* (2018) on an Agilent 1260 series HPLC system (Agilent Technologies) coupled to a tandem mass spectrometer API5000 (SCIEX, Darmstadt, Germany). Since D_6-labeled JA and D_6-labeled JA-Ile standards (HPC Standards GmbH, Cunnersdorf, Germany) contained 40% of the corresponding D_5-labeled compounds, the sum of the peak areas of D_5- and D_6-compound was used for quantification. Details of the instrument parameters and response factors for quantification are shown in Supplementary Table S3.

Indolacetic acid was quantified using the same LC-MS/MS system with the same chromatographic conditions but using positive mode ionization with an ion spray voltage at 5500 eV. Multiple reaction monitoring was used to monitor analyte parent ion→product ion fragmentations as follows: m/z 176→130 (collision energy (CE) 19 V; declustering potential (DP) 31 V) for indolacetic acid (IAA); m/z 181→133 + m/z 181→134 + m/z 181→135 (CE 19 V; DP 31 V) for D_5-indolacetic acid.

Anthocyanin and total phenolic content quantification

Anthocyanin quantification was measured as previously described (Agudelo-Romero *et al.*, 2013). Total relative anthocyanin concentration was expressed as absorbance value at 520 nm per gram freeze-dried weight.

Total phenolic content was measured using the Folin–Ciocalteau colorimetry method and a gallic acid calibration curve ranging from 12.5 to 125 µg ml^{-1} (Singleton and Rossi, 1965). Phenolics were extracted from 50 mg of lyophilized grape berry samples in ultra-pure water and centrifuged at 15 000 *g* for 30 min. Twenty microliters of the extract was added to diluted Folin–Ciocalteu reagent (1:10). Upon 10 min incubation, 800 µl of 7.5% (w/v) sodium carbonate was added to the reaction, incubated for 30 min, and absorbance measured at 743 nm. Total phenolic content was expressed as gallic acid equivalents (GAE, mg) per mg freeze-dried weight.

Protein extraction and phenylalanine ammonia lyase enzymatic assay

Protein extraction from grape berry powder was performed as described by Conde *et al.* (2016), with minor alterations. Briefly, 1 g of deep-frozen grape berry powder was mixed with 2 ml of extraction buffer and centrifuged at 18 000 *g* for 20 min at 4°C. Supernatant was used for further assays. Protein extraction buffer contained 50 mM Tris–HCl pH 8.8, 5 mM $MgCl_2$, 1 mM EDTA pH, 1 mM phenylmethylsulfonyl fluoride, 5 mM dithiothreitol and 1% (w/v) PVPP. Total protein content of each extract was determined by the Bradford assay (Bradford, 1976), using bovine serum albumin as standard.

Phenylalanine ammonia lyase (PAL) enzymatic activity was measured in a reaction mixture containing 200 µl of protein extract, 500 µl 250 mM Tris–HCl pH 8.8, and 250 µl substrate (40 mM L-phenylalanine, 100 mM Tris–HCl pH 8.8) and was incubated at 37 °C for 30 min. The rate of conversion of L-phenylalanine to cinnamic acid was monitored spectrophotometrically at 290 nm each 10 min (ε=17400 M^{-1} cm^{-1}). The reaction was initiated by the addition of L-phenylalanine.

Statistical analysis

Statistical analysis of metabolomics data was performed using log_2-transformed response ratios and included Student's *t*-test, one- and two-way ANOVA, Kruskal–Wallis and Wilcoxon rank-sum tests. For multiple comparisons, the Benjamini–Hochberg correction was used, which defines a sequential *P*-value procedure that controls the expected proportion of falsely rejected hypotheses – the FDR. Principal component analysis was performed applying the MetaGeneAlyse web application (v.1.7.1; http://metagenealyse.mpimp-golm.mpg.de) and the R function prcomp to the log_2-transformed response ratios with missing value substitution, log_2=0. Heatmaps were designed using the R package ComplexHeatmap (Gu *et al.*, 2016). Venn diagrams were designed using Venny 2.1 web application (v. 2.1.0; http://bioinfogp.cnb.csic.es/tools/venny/).

Results

Phenotypic assessment and evaluation of main ripening parameters in powdery mildew-infected and control grape berries

In order to study the effect of powdery mildew infection on grape berry physiology, infected and healthy berry samples were collected at two ripening stages, green (EL33) and early véraison (EL35), according to the modified E-L system (Fig. 1; Coombe, 1995). The EL33 stage is characterized by green and firm berries, with low sugar content, and EL35, which corresponds to the onset of ripening, is characterized by berry softening, anthocyanin accumulation, and increase in sugar content (Conde *et al.*, 2007). Infected and control samples were distinguished by visual inspection and fungal biomass accumulation evaluated by real-time PCR (Supplementary Fig. S1).

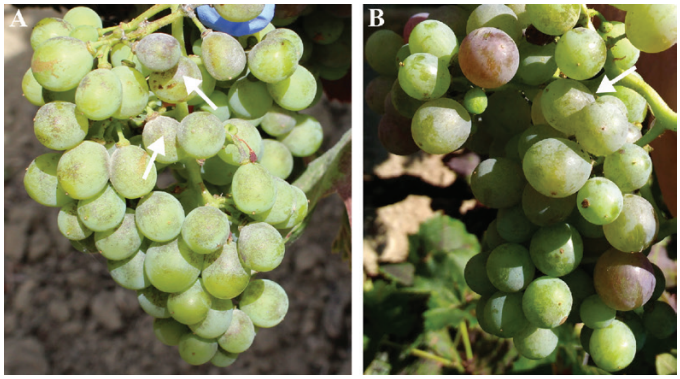

Fig. 1. Clusters of *Vitis vinifera* cv. Carignan grapes naturally infected with powdery mildew (*Erysiphe necator*) at (A) EL33 and (B) EL35 developmental stages.

Berry weight and content of main sugars, organic acids, and anthocyanins were analysed to evaluate the effect of PM in the main parameters of fruit ripening (Fig. 2). PM infection led to a higher accumulation of anthocyanins at the green stage; however, no significant changes were observed for berry weight, sugar, and organic acids between control and infected berries. At early véraison stage, an increase in anthocyanins and glucose and fructose content was observed in both conditions. These results suggest that PM infection caused a minor effect on the main ripening parameters.

Metabolic profiling of control and infected berries revealed a substantial reprogramming of fatty acid metabolism

Metabolic profiling of control and infected berries was performed by GC-EI/TOF-MS, which allowed the relative quantification of 100 metabolites belonging to several classes of compounds, such as fatty acids, sugars, and phenylpropanoids (Supplementary Table S4). Volatile compounds (23) were included by SPME and GC-EI/QUAD-MS (Supplementary Table S4). Normalized response data were used for principal component analysis. The two major principal components explained 37.65% of the variability, showing a good separation between control and infected berries and also between developmental stages (Supplementary Fig. S2). Thirty-six metabolites showed differential content comparing either infected and control samples or green and véraison stages (Fig. 3; Supplementary Table S4). Additionally, 20 metabolites were identified as potential positive markers of infection (Fig. 4; Supplementary Table S4), i.e. metabolites that were significantly increased (response ratio ≥1.5 and $P \leq 0.05$) or detected only in infected berries. These metabolites included fatty acids (eicosanoic, docosanoic, and tetracosanoic acids), fatty alcohols (eicosan-1-ol, docosan-1-ol, and octadecan-1-ol), lipids (α-tocopherol), phenylpropanoids (resveratrol and catechins), phenolic acids (gallic acid), sugar conjugates (4-hydroxyphenyl-β-glucopyranoside and salicylic acid-glucopyranoside), and an unidentified compound (A255011).

Regarding fatty acids, several saturated long-chain fatty acids and fatty alcohols were present in a significantly higher amount in infected berries in comparison with control (Fig. 3). Eicosanoic acid (arachidic acid), docosanoic acid (behenic acid), and tetracosanoic acid were accumulated in infected berries at both stages (Fig. 4). Eicosanoic acid was identified as a quantitative marker of PM presence in grape berries (Petrovic *et al.*, 2017). Hexacosanoic acid, octacosanoic acid, and pentacosanoic acid were also responsive to infection but only at the green stage (Fig. 3). The fatty alcohol derived from eicosanoic acid (*n*-eicosan-1-ol) was only detected in infected berries (Fig. 4). Concerning other acids, fumaric acid, an intermediate metabolite in the citric acid cycle, was present in a lower amount in infected berries at EL33 in comparison with control (Fig. 3).

Concerning secondary metabolites, gallic acid, catechins, α-tocopherol, and the phytosterol stigmasterol were present in higher quantity in infected berries than in control berries at EL33 and/or EL35 stages (Fig. 3) while resveratrol was only identified in infected berries (Fig. 4), confirming other studies (Piermattei *et al.*, 1999). Relative to terpene metabolism, putative ursolic/oleanolic acid and cycloartenol were present in lower amounts in infected berries at EL35 and both stages, respectively (Fig. 3).

Regarding volatile compounds, four metabolites were identified as infection responsive. Limonene, undecane, and phenylacetaldehyde were accumulated less in infected berries at the véraison stage than in control berries (Fig. 3). On the other hand, benzaldehyde was accumulated after infection at the green stage (Fig. 3).

These results indicate a substantial metabolic reprogramming in berries upon infection with *E. necator*, involving fatty acid and phenylpropanoid metabolism.

Transcriptional profiling of infected and control grape berry samples

RNA-seq analysis was carried out to access the expression profiles of PM-infected and control berries at the EL33 and EL35 stages. An average of 46 468 679±2 280 892 raw reads were obtained per sample and aligned to the concatenated grapevine PN40024 reference genome and *E. necator* C-strain scaffolds; 86.5±8.0% were retained after filtering (Supplementary Table S2). RNA-seq data revealed the expression of 25 381 grapevine genes (84.7% of total annotated genes) across all berry samples; 4275 genes (14.6%) were identified as differentially expressed due to infection (1472) and/or véraison-responsive (3385) (Supplementary Table S5; Supplementary Fig. S3). DEGs were identified using edgeR with a TMM normalization factor close to 1 (Supplementary Table S2). A multidimensional scaling plot

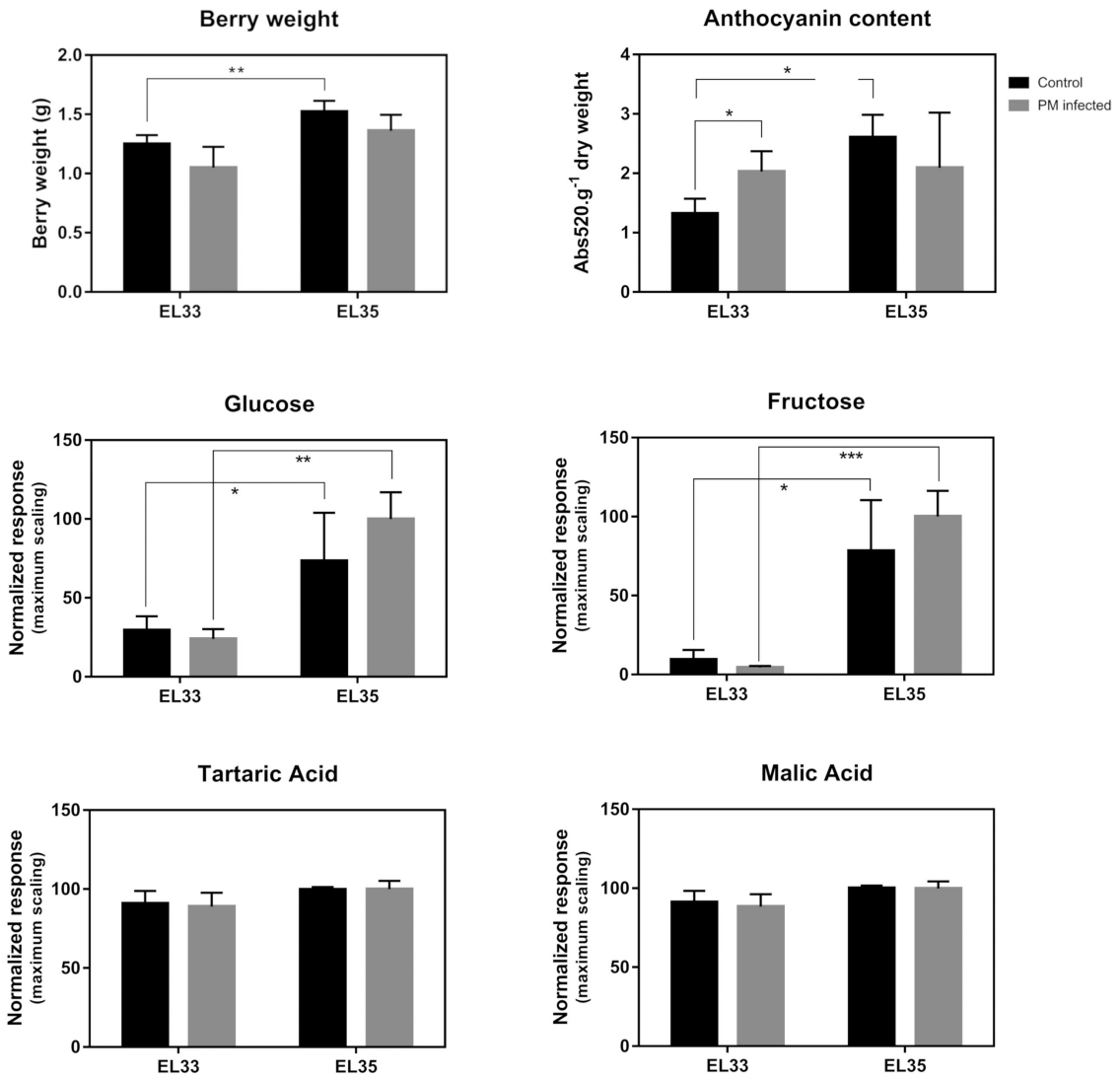

Fig. 2. Phenotypic and metabolic characterization of powdery mildew-infected (PM) and control grape berries at developmental stages EL33 (green) and EL35 (véraison): berry weight, anthocyanin content (absorbance at 520 nm g^{-1} of freeze-dried material), and relative quantification of glucose, fructose, tartaric acid, and malic acid (Supplementary Table S4). Bars and whiskers represent means and standard deviation (SD). Significance (*P*-value) of indicated pairwise comparisons was assessed by Student's *t*-test: $^{*}P \leq 0.05$, $^{**}P \leq 0.01$, $^{***}P \leq 0.001$.

showed good separation among control and infected berries and developmental stages (Supplementary Fig. S4). RNA-seq data also supported the absence of *E. necator* infection in control samples, shown by the residual number of reads mapped into the *E. necator* C-strain scaffolds (Supplementary Table S2). Additionally, these RNA-seq data were validated by real-time PCR analysis (Supplementary Figs S5, S6).

Functional enrichment analysis

Functional enrichment analysis of up- and down-regulated transcripts was performed (Fig. 5; Supplementary Table S6) based on functional categories defined by Grimplet *et al.* (2012); two comparisons were considered: transcriptional changes between control and infected berries (Fig. 5) and during ripening (EL35 compared with EL33; Supplementary Fig. S7).

Genes that were up-regulated in infected berries at both stages (Fig. 5) are mainly related to signaling pathways and protein kinases, secondary metabolism (including phenylpropanoids, stilbenoids, and lignin biosynthesis), stress response (biotic stress response, plant–pathogen interaction, oxidative stress), hormone signaling (in particular salicylic acid signaling), nitrogen metabolism, phytoalexin biosynthesis, NBS-LRR superfamily, and WRKY transcription factor family. Activation of secondary metabolism and defense/stress responses was also observed in *V. vinifera* leaves infected with *E. necator* (Fung *et al.*, 2008; Fekete *et al.*, 2009).

Functional categories enriched as up-regulated only at the EL33 stage included genes involved in transport and secondary metabolism (aromatic compound glycosylation, flavonoid, and isoflavonoid biosynthesis). They also included

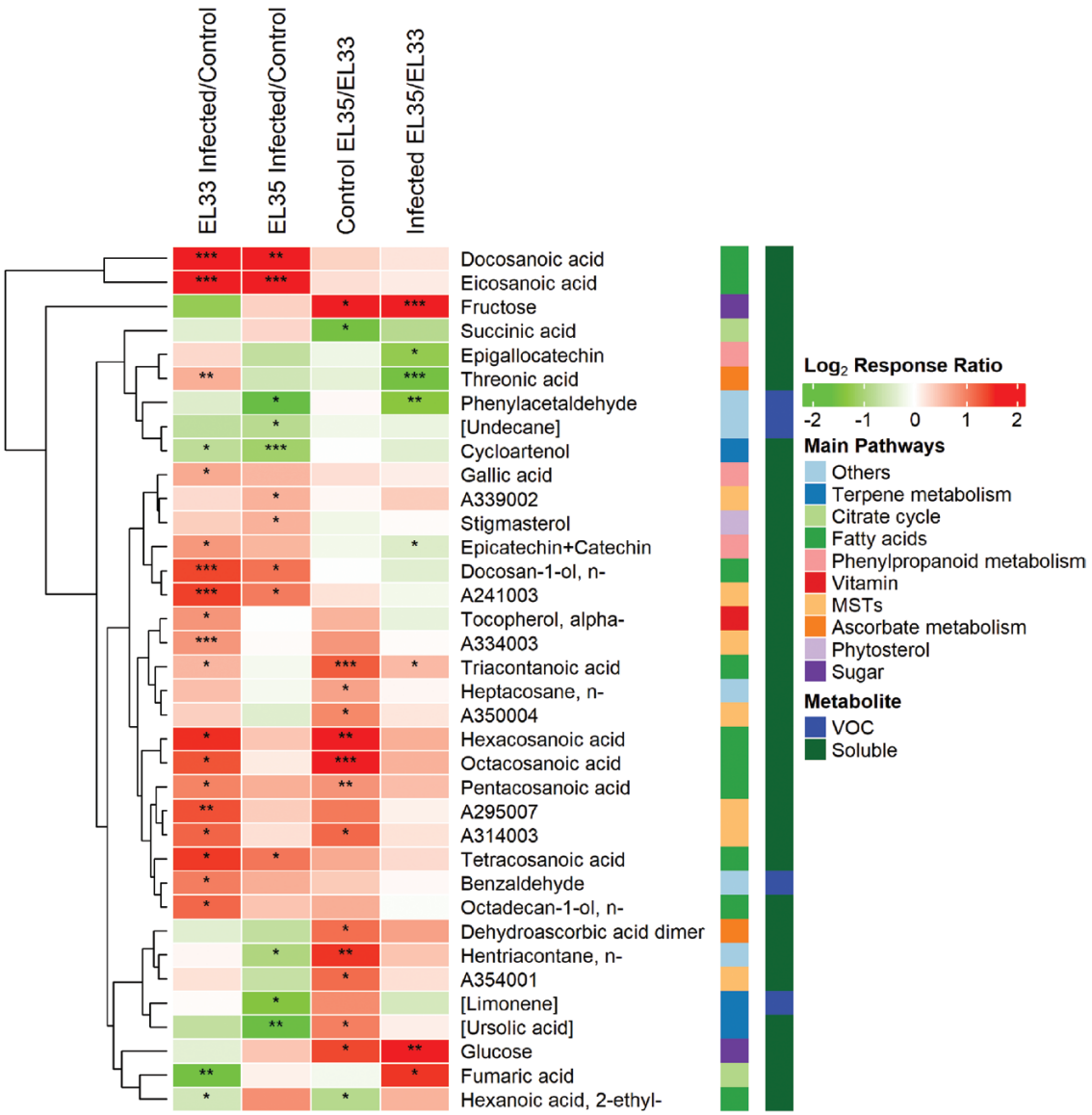

Fig. 3. Metabolic analysis of infection- and véraison-responsive metabolites from powdery mildew-infected and control berries at the green (EL33) and véraison (EL35) developmental stages. Metabolites that were significantly increased or decreased in at least one of the pairwise comparisons with response ratio ≥1.5 and $P \leq 0.05$ (statistical tests and analyses of variation in Supplementary Table S4) are presented by a heatmap. Metabolites present only in infected berries were not included. Response ratios were $\log_2$-transformed (see scale) and hierarchically clustered using Euclidean distance and complete linkage. Asterisks indicate statistical significance (Student's *t*-test: $^{*}P \leq 0.05$, $^{**}P \leq 0.01$, $^{***}P \leq 0.001$). Square brackets indicate metabolites that were identified only by mass spectral match. MTS, mass spectral tag.

genes belonging to MYB transcription factor family, ABA-mediated and brassinosteroid-mediated signaling (Fig. 5; Supplementary Table S6). Additionally, aromatic amino acid metabolism (phenylalanine and tyrosine biosynthesis), lipid metabolism (glycerolipid catabolism), and subtilase-mediated proteolysis were categories enriched only at the EL35 stage (Fig. 5; Supplementary Table S6).

At the green stage, very few categories were enriched as down-regulated (116 genes; Supplementary Table S5); they were associated with cell growth, cell wall organization and biogenesis (including cell wall metabolism, modification, and pectin metabolism,), cellular metabolism (cytochrome P450 oxidoreductase), and carbohydrate metabolism (Fig. 5; Supplementary Table S6). Moreover, no functional category was enriched at the véraison stage since only 28 genes were down-regulated (Fig. 5; Supplementary Tables S5, S6).

Modulation of genes involved in biotic stress responses indicates an activation of defensive signaling events in non-ripe infected fruits

Genes involved in biotic stress responses were vastly modulated in response to infection, namely genes encoding protein and receptor-like kinases (Table 1; Supplementary Table

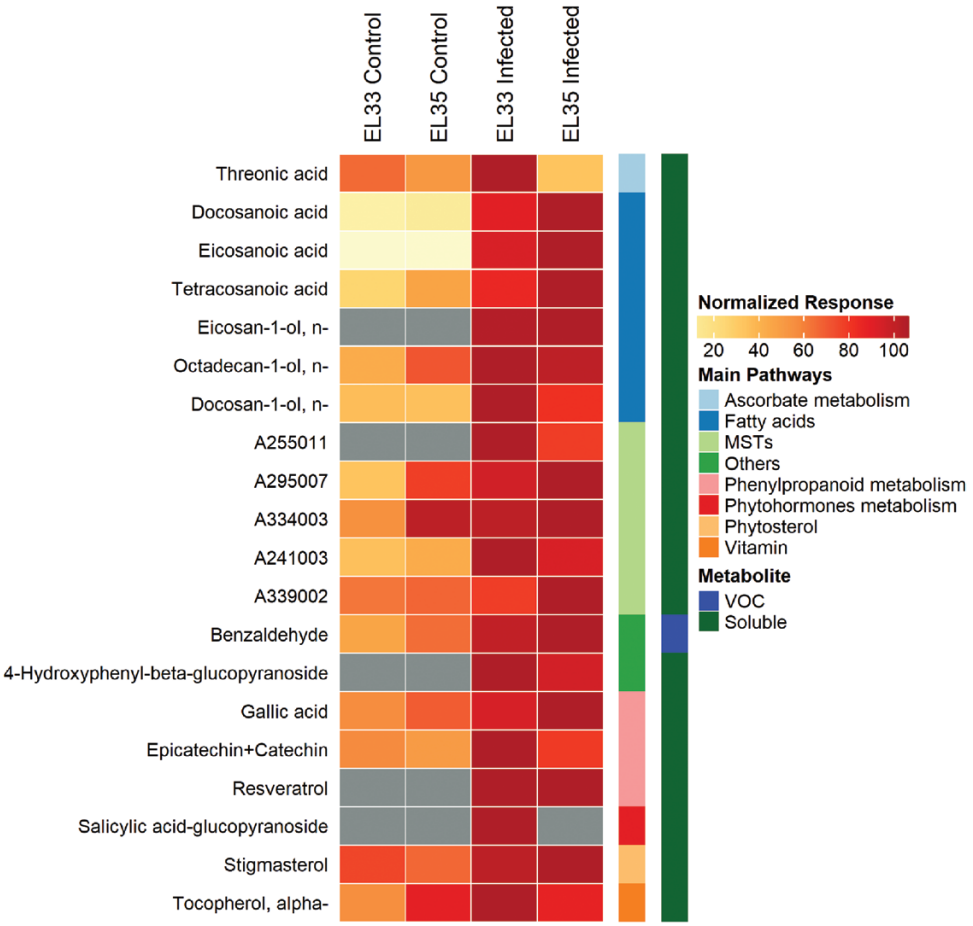

Fig. 4. Potential positive markers of powdery mildew infection of berries of *V. vinifera* cv. Carignan at EL33 and EL35 stages. Metabolites selected were either significantly increased after infection at one or both developmental stages (response ratio ≥1.5 and $P \leq 0.05$, Student's *t*-test) or only detected in infected berries. The heatmap represents normalized responses in a two-color scale: low, light orange; high, dark red; grey boxes indicate non-detected metabolites. MTS, mass spectral tag; VOC, volatile organic compounds.

S5). Several genes encoding PAMPs receptors were activated in response to PM, including *Wall-associated receptor kinase* (*WAK*), *Brassinosteroid insensitive 1-associated receptor kinase 1* (*BAK1*), *Flagellin-sensitive 2* (*FLS2*), and the gene for chitin elicitor-binding CEBIP LysM domain-containing (LysM protein) (Table 1). Many genes belonging to the NBS-LRR superfamily, and other R proteins were overexpressed in response to infection at both stages (Table 1; Supplementary Table S5). Moreover, genes encoding Avr9/Cf-9-induced proteins were responsive to infection and were reported to regulate the hypersensitive response in grapevine leaves (Rowland *et al.*, 2005; Toth *et al.*, 2016). Genes encoding two mitogen-activated protein kinases (MAPKs), MAPKKK5 and MAP4K α1, were induced in infected berries at the green stage (Table 1; Supplementary Table S5).

Additionally, several other genes widely described as involved in biotic stress responses were activated such as those coding for PR-10, calmodulin-binding proteins, cyclic nucleotide-gated ion channel, and glutathione *S*-transferases (Table 1; Supplementary Table S5).

Myb and WRKY were the transcription factor gene families most responsive to PM infection (Table 1; Supplementary Table S5). Other transcription factor families with PM-responsive members, particularly at the green stage, were the *Lateral Organ Boundary* (*LOB*) *domain* family and the zinc finger C3HC4 family (Table 1; Supplementary Table S5). Several *LOB domain* genes were previously associated with response to powdery mildew (Grimplet *et al.*, 2017).

Despite the substantial activation of genes involved in defense response, six *Mildew Locus O* (*MLO*) genes (susceptibility genes, *S*-genes) were also up-regulated in infected berries at both stages (Table 1; Supplementary Table S5).

Genes involved in primary and secondary metabolisms are extensively modulated upon infection

Several genes involved in primary metabolism were responsive to PM infection. Nitrogen metabolism (enriched as up-regulated at EL33) included genes coding for ammonium transporters and copper amine oxidase (Table 1; Supplementary Table S5),

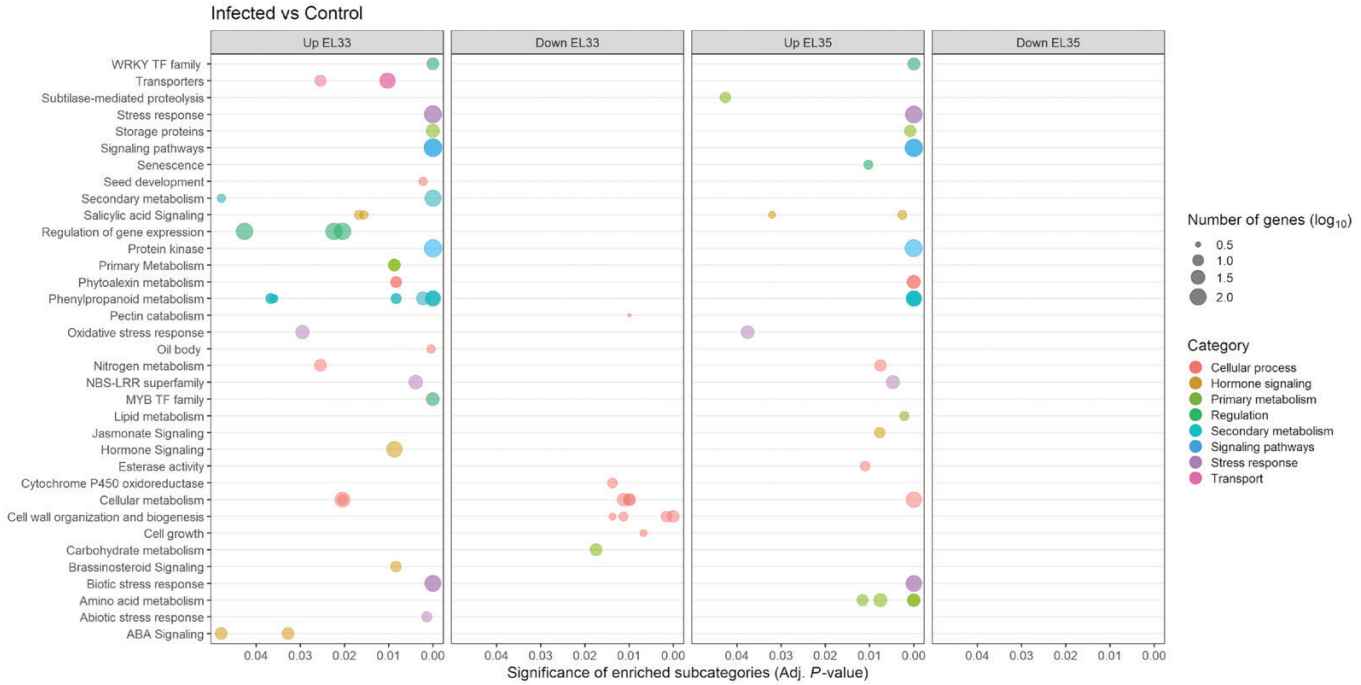

Fig. 5. Enriched functional subcategories (adjusted $P \leq 0.05$) in response to PM infection (infection vs control). Circle size represents the number of genes ($\log_{10}$) for each functional subcategory. Complete dataset in Supplementary Table S6.

suggesting a modulation of host nitrogen transport and metabolism that might eventually be induced by the fungus.

Although the carbohydrate metabolism category was enriched as down-regulated in green infected berries due to an over-representation of genes involved in cell wall metabolism (Table 1; Supplementary Table S6), several genes involved in sugar metabolism were up-regulated and may play an important role in supplying energy and/or precursors for defensive mechanisms. These included genes related to glycolysis and gluconeogenesis, monosaccharide metabolism, starch and sucrose metabolism, trehalose metabolism, and polyol and sugar transport (Table 1; Supplementary Table S5).

Moreover, genes encoding enzymes involved in fatty acid biosynthesis, glycerophospholipids metabolism, and lipid transport were also responsive to infection (Table 1; Supplementary Table S5), which is in accordance with the accumulation of fatty acids revealed in the metabolic profiling.

Secondary metabolism was also extensively reprogrammed upon infection involving activation of phytoalexin and phenylpropanoid metabolisms (Fig. 6). The activation of resveratrol synthesis in response to PM infection (Schnee *et al.*, 2008) was supported by up-regulation of genes encoding stilbene synthases (Table 1; Fig. 6; Supplementary Table S5). Reprogramming of the phenylpropanoid pathway was also observed in leaves of susceptible *V. vinifera* cv. Cabernet Sauvignon (Fung *et al.*, 2008) and involved up-regulation of genes coding for the enzyme PAL (Table 1; Fig. 6). Nevertheless, its total activity and total phenolic content showed no significant differences between infected and control berries (Supplementary Fig. S8) ultimately due to post-transcriptional regulation and/or specific dynamics of fluxes of phenylpropanoid metabolites. Flavonoid, hydroxycinnamate, and lignin biosynthetic pathways were also stimulated in response to PM (Table 1; Fig. 6; Supplementary Table S5).

Modulation of genes involved in hormonal metabolism highlights the central role of salicylic acid signaling in response to powdery mildew

The data indicated a strong reprogramming of hormonal metabolism upon infection.

Regarding the salicylic acid (SA) pathway, an overexpression of the *EDS1* and *PR-1* genes was observed upon infection at both stages (Table 1). *SAMT* and *SAG101* genes involved in SA metabolism (Feys *et al.*, 2005) were also up-regulated (Table 1; Supplementary Table S5).

Concerning jasmonic acid (JA) metabolism, genes encoding methyl jasmonate esterase, lipoxygenases (LOX), and an allene oxide synthase (AOS) were up-regulated in green infected berries (Table 1; Supplementary Table S5). Additionally, one gene belonging to the cytochrome P450 (CYP94) family was modulated (Table 1). Members of the CYP94 family are involved in the oxidation of the bioactive form of JA, jasmonoyl-L-isoleucine (JA-Ile; Koo *et al.*, 2011, 2014). Several members of the AP2 transcription factor family, including ethylene-responsive factors (ERF) genes, were also activated in infected berries (Table 1; Supplementary Table S5).

Table 1. Selection of *Vitis vinifera* infection-responsive genes in powdery mildew (PM)-infected and control grape berries (fold-change considering an FDR of ≤0.05 and a fold change of ≥ 2 or ≤ –2)

Gene ID	Fold-change				Functional annotation	Functional category
	EL33 (PM vs control)	EL35 (PM vs control)	Control (EL35 vs EL33)	PM infected (EL35 vs EL33)		
Signaling (kinases, receptors)						
VIT_19s0014g04060	18.6	5.2			ARK3 (arabidopsis receptor kinase 3)	Protein kinase
VIT_16s0148g00100	86.0	16.5			Brassinosteroid insensitive 1-associated receptor kinase 1	PAMPs receptor
VIT_03s0038g03220		2.7	–3.2		Chitin elicitor-binding CEBIP LysM domain-containing	PAMPs receptor
VIT_04s0008g00330	45.6	7.5			Clavata1 receptor kinase (CLV1)	PAMPs receptor
VIT_00s2485g00010	32.7	15.3			CRK10 (cysteine-rich RLK10)	Protein kinase
VIT_14s0066g00760	11.8	6.7			Disease resistance protein (NBS-LRR class)	NBS-LRR superfamily
VIT_07s0197g00130		2.8			Disease resistance protein (TIR-NBS-LRR class)	NBS-LRR superfamily
VIT_16s0050g01980	5.5	6.6			EIX receptor 2	NBS-LRR superfamily
VIT_01s0010g00380	54.8	9.0			FLS2 (flagellin-sensitive 2)	PAMPs receptor
VIT_09s0002g03010	47.3	11.8		–4.3	FRK1 (FLG22-induced receptor-like kinase 1)	Protein kinase
VIT_00s0400g00020	4.0	4.7			HcrVf1 protein	NBS-LRR superfamily
VIT_12s0035g00150	8.9	3.8		–2.1	Leucine-rich repeat receptor-like kinase	Protein kinase
VIT_18s0001g13590	50.1				Leucine-rich repeat protein kinase	Protein kinase
VIT_01s0127g00690	13.6			–8.8	MAP4K α1	MAPK cascade
VIT_18s0001g11240	3.4				MAPKKK5 (mitogen-activated protein kinase kinase kinase 5)	MAPK cascade
VIT_18s0089g00450	3.1				R protein L6	R protein
VIT_15s0024g00400	3.2	6.5			R protein MLA10	R protein
VIT_00s0226g00080	28.6	17.0			R protein PRF disease resistance protein	R protein
VIT_00s0258g00130	60.4	14.5			Receptor kinase homolog LRK10	Protein kinase
VIT_16s0148g00370	191.3	127.2			Receptor serine/threonine kinase	Protein kinase
VIT_10s0003g02010	57.3				RKF1 (receptor-like kinase in flowers 1)	Protein kinase
VIT_19s0014g00810	6.7	5.5	–2.9	–3.6	RKF1 (receptor-like kinase in flowers 1)	Protein kinase
VIT_19s0014g04080	16.1	165.6			Serine/threonine-protein kinase receptor ARK3	Protein kinase
VIT_12s0028g03520	79.0	39.1			S-receptor kinase	Protein kinase
VIT_17s0000g04400	33.8	12.6			Wall-associated kinase 1 (WAK1)	PAMPs receptor
Biotic stress response						
VIT_12s0028g02280	4.7			–3.0	Calcium-dependent protein kinase 13 CPK13	Calcium sensors and signaling
VIT_14s0030g02150	477.5	135.5		–4.6	Calmodulin	Calcium sensors and signaling
VIT_17s0000g03370	9.5	22.3			Calmodulin-binding protein	Calcium sensors and signaling
VIT_06s0004g02670	2.7				Cyclic nucleotide-gated ion channel 15	Stress response
VIT_08s0040g01770	4.4	2.9			Cyclic nucleotide-gated ion channel 15	Stress response
VIT_08s0040g00920	130.2	34.1		–7.4	Glutathione *S*-transferase 25 GSTU7	Oxidative stress response
VIT_12s0035g02100	96.2				Glutathione *S*-transferase Z1 GSTZ1	Oxidative stress response
VIT_06s0004g03120	136.9	18.9		–4.8	MLO-like protein 3	Susceptibility
VIT_05s0077g01530	15.0	5.9			Pathogenesis protein 10 (*Vitis vinifera*)	PR protein

Table 1. Continued

Gene ID	Fold-change				Functional annotation	Functional category
	EL33 (PM vs control)	EL35 (PM vs control)	Control (EL35 vs EL33)	PM infected (EL35 vs EL33)		
VIT_08s0058g00990	17.5	15.9		−4.9	Peroxidase	Oxidative stress response
VIT_14s0068g01920		14.1			Peroxidase	Oxidative stress response
VIT_02s0025g04270		12.6			Thaumatin	Stress response
VIT_02s0025g04230	7.2	14.3			Thaumatin (*Vitis vinifera*)	Stress response
Transcription factors						
VIT_08s0056g01650	19.9			−15.8	Lateral organ boundaries domain protein 20 (LBD20)	LBD transcription factor family
VIT_16s0050g00050	130.6				Myb domain protein 18	MYB transcription factor family
VIT_19s0085g00050	27.5	14.8			Myb domain protein 58	MYB transcription factor family
VIT_00s1624g00010	51.9			−8.9	Myb family	MYB transcription factor family
VIT_13s0067g01880		5.6		4.0	Other LOB domain-containing protein ASL5	LBD transcription factor family
VIT_13s0067g03130		12.0		4.2	WRKY DNA-binding protein 55	WRKY transcription factor family
VIT_08s0058g01390	13.4	11.1			WRKY DNA-binding protein 70	WRKY transcription factor family
VIT_14s0068g01770	66.3				WRKY DNA-binding protein 75	WRKY transcription factor family
VIT_07s0031g00380	95.0			−11.3	Zinc finger (C3HC4-type ring finger)	Zinc finger C3HC4 transcription factor family
VIT_12s0028g02530	17.3	8.4			Zinc finger (C3HC4-type ring finger)	Zinc finger C3HC4 transcription factor family
Cell wall metabolism						
VIT_15s0046g01580	91.6				Acidic chitinase III	Carbohydrate metabolism
VIT_15s0046g01570		2.8	−3.0		Acidic endochitinase (CHIB1)	Carbohydrate metabolism
VIT_08s0007g06060	15.6	19.7			β-1,3-Glucanase	β-1,3-Glucan catabolism
VIT_01s0137g00430	−3.1			3.2	Cellulase	Cell wall organization and biogenesis
VIT_00s0531g00060	229.6				Cellulose synthase CSLE1	Cellulose biosynthesis
VIT_02s0025g01920	5.8	15.0	−5.5	−2.1	Cellulose synthase CSLG3	Cellulose biosynthesis
VIT_05s0094g00320	53.5	124.6			Chitinase, class IV (*Vitis vinifera*)	Carbohydrate metabolism
VIT_00s2526g00010	7.8	4.3			Endo-1,4-β-glucanase korrigan (KOR)	Cellulose catabolism
VIT_13s0067g02930	−9.1			15.4	Expansin (*Vitis labrusca* × *Vitis vinifera*) EXPA8	Cell growth
VIT_16s0039g00260	−8.6			5.2	Pectate lyase	Pectin catabolism
VIT_16s0022g00940	−16.6		6.0	94.0	Pectinesterase PME3	Pectin modification
VIT_06s0061g00550	−17.2			62.4	Xyloglucan endotransglucosylase/hydrolase 32	Xyloglucan modification
Cuticle biosynthesis						
VIT_04s0008g06000	−4.7		3.1	14.0	Ethylene-responsive transcription factor ERF003	ERF subfamily transcription factor
VIT_05s0029g00480		−2.1		−2.8	Eceriferum 2 (CER2)	Cuticle biosynthesis
VIT_09s0018g01360	2.9				Cuticle protein	Cuticle biosynthesis
Nitrogen metabolism						
VIT_08s0058g00140	31.6	5.8		−5.5	Ammonium transporter 2	Ammonium transport
VIT_08s0007g03240	4.4			−5.3	Carbonic anhydrase precursor	Nitrogen metabolism
VIT_05s0020g03280	80.2	43.4			Copper amine oxidase	Polyamine metabolism

Table 1. Continued

Gene ID	Fold-change				Functional annotation	Functional category
	EL33 (PM vs control)	EL35 (PM vs control)	Control (EL35 vs EL33)	PM infected (EL35 vs EL33)		
VIT_07s0005g00530	42.7				NADH glutamate synthase	Glutamate metabolism
VIT_01s0127g00070	6.1	4.2			Nitrate transporter 2.5	Nitrate transport
VIT_03s0063g01250	3.2				Nodulin 1A, senescence-associated	Nitrogen assimilation
VIT_08s0007g04860	3.3			–4.9	Nodulin family protein	Nitrogen assimilation
VIT_13s0019g05070	30.4	11.5			Nodulin family protein	Nitrogen assimilation
Carbohydrate metabolism						
VIT_17s0000g05870	9.8				Aldose 1-epimerase protein	Glycolysis/gluconeogenesis
VIT_03s0063g00400		2.0			α-Amylase/1,4-α-D-glucan glucanohydrolase	Starch and sucrose metabolism
VIT_10s0071g01120	26.3			–42.0	α-Galactosidase	Monosaccharide metabolism
VIT_02s0025g00180	3.0			–3.6	Bisphosphoglycerate mutase	Glycolysis/gluconeogenesis
VIT_19s0015g01720	11.1				Fructose-bisphosphate aldolase, cytoplasmic isozyme 1	Glycolysis/gluconeogenesis
VIT_00s0895g00010	19.4			–3.2	Glucan-1,3-β-glucosidase	Starch and sucrose metabolism
VIT_16s0013g01950		3.7			Hexose transporter (*Vitis vinifera*)	Sugar transport
VIT_10s0003g03930	2.6	1.8	–1.9	–2.7	Inositol transporter 2	Polyol transport
VIT_15s0048g00640	407.6			–15.9	L-Lactate dehydrogenase	Glycolysis/gluconeogenesis
VIT_04s0044g00210	162.4		14.6		Mannitol dehydrogenase	Monosaccharide metabolism
VIT_03s0063g02250	5.1	2.6		–3.6	Polyol transporter 5	Polyol transport
VIT_12s0057g00130	64.7			–11.1	Sucrose synthase 2	Starch and sucrose metabolism
VIT_05s0020g03140	9.3				Sugar transporter 13	Sugar transport
VIT_01s0011g05960	2.1				Trehalose-phosphatase	Trehalose metabolism
Lipid metabolism						
VIT_18s0001g04750	48.5			–9.1	Acetylcholinesterase	Glycerophospholipids metabolism
VIT_04s0079g00790		6.0			Acyl-CoA synthetases (acyl-activating enzyme 11)	Fatty acid metabolism
VIT_07s0005g01760		12.7			Glycerol-3-phosphate acyltransferase 3 (AtGPAT3)	Glycerophospholipids metabolism
VIT_14s0219g00280	3.7			–4.8	Glycerol-3-phosphate dehydrogenase (NAD^+)	Glycerophospholipids metabolism
VIT_12s0028g01180	32.8		5.7		Non-specific lipid-transfer protein	Lipid transport
VIT_06s0004g01250	33.9			–9.3	Omega-6 fatty acid desaturase, endoplasmic reticulum (FAD2)	Fatty acid metabolism
VIT_14s0108g00520	452.4		519.9		Protease inhibitor/seed storage/lipid transfer protein (LTP)	Lipid transport
VIT_12s0028g02000	2.4		–2.0	–3.1	Triacylglycerol lipase	Glycerophospholipids metabolism
Secondary metabolism						
VIT_03s0017g02110	4.3	6.5	–3.4		Anthocyanidin 3-*O*-glucosyltransferase	Anthocyanin biosynthesis
VIT_09s0018g01190	8.2	6.5	–2.2	–2.8	Anthranilate *N*-benzoyltransferase	Phytoalexin biosynthesis
VIT_10s0003g00900	3.2			–2.3	Anthranilate *N*-hydroxycinnamoyl/benzoyltransferase	Phytoalexin biosynthesis

Table 1. Continued

Gene ID	Fold-change				Functional annotation	Functional category
	EL33 (PM vs control)	EL35 (PM vs control)	Control (EL35 vs EL33)	PM infected (EL35 vs EL33)		
VIT_16s0098g00850	2.1	1.9	−1.8	−2.0	Caffeic acid *O*-methyltransferase	Phenylpropanoid biosynthesis
VIT_03s0063g00140	10.4	11.6	−3.3	−2.9	Caffeoyl-CoA *O*-methyltransferase	Phenylpropanoid biosynthesis
VIT_13s0067g03820	2.6				Chalcone-flavonone isomerase (chalcone isomerase)	Flavonoid biosynthesis
VIT_09s0070g00240	4.9	5.9	−2.9	−2.4	Cinnamoyl-CoA reductase	Lignin biosynthesis
VIT_07s0031g01380	53.4	29.2			Ferulate 5-hydroxylase	Phenylpropanoid biosynthesis
VIT_07s0031g01370	25.8	3.8		−5.4	Flavonoid 3-monooxygenase	Flavonoid metabolism
VIT_13s0047g00210	3.7	3.2			Flavonol synthase	Flavonoid metabolism
VIT_12s0028g01880	150.1	9.9		−9.8	Isoflavone methyltransferase/orcinol *O*-methyltransferase 1 OOMT1	Flavonoid metabolism
VIT_07s0031g03070	417.9			−18.4	Isoflavone reductase	Flavonoid metabolism
VIT_08s0040g01710	7.8	9.0	−2.9	−2.6	Phenylalanine ammonia-lyase	Phenylpropanoid biosynthesis
VIT_08s0058g00790	19.9	13.0			Secoisolariciresinol dehydrogenase	Lignan biosynthesis
VIT_16s0100g01010	18.7	10.8			Stilbene synthase	Stilbene biosynthesis
VIT_06s0004g08150	3.3	1.8		−2.4	*trans*-Cinnamate 4-monooxygenase	Phenylpropanoid biosynthesis
VIT_05s0062g00350	56.5				UDP-glucose:flavonoid 7-*O*-glucosyltransferase	Flavonoid biosynthesis
Hormonal metabolism						
Salicylic and jasmonic acid						
VIT_18s0001g11630	2.4		10.1	3.3	Allene oxide synthase	Jasmonate metabolism
VIT_07s0141g00890	16.7	24.7			CYP94A1	Jasmonate metabolism
VIT_17s0000g07370	2.7	3.3			EDS1 (enhanced disease susceptibility 1)	Salicylic acid-mediated signaling
VIT_17s0000g07420		6.4	−2.9		EDS1 (enhanced disease susceptibility 1)	Salicylic acid-mediated signaling
VIT_06s0004g01500	45.7				Lipoxygenase (LOX2)	Jasmonate metabolism
VIT_06s0004g01480	6.1			−4.5	Lipoxygenase LOX1	Jasmonate metabolism
VIT_00s0253g00170	33.9				Methyl jasmonate esterase	Jasmonate metabolism
VIT_03s0088g00710	79.4	23.6			Pathogenesis-related protein 1 precursor (PRP 1)	Salicylic acid-mediated signaling
VIT_01s0011g05920	4.7				*S*-Adenosyl-L-methionine:salicylic acid carboxyl methyltransferase	Salicylic acid metabolism
VIT_14s0066g01830	3.8	4.3			SAG101 (senescence-associated gene 101)	Salicylic acid-mediated signaling
Auxin						
VIT_13s0067g00330	3.8				AUX1 auxin influx carrier protein	Auxin transport
VIT_12s0057g00420	6.7	6.0			Auxin-responsive protein AIR12	Auxin signaling
VIT_07s0005g04380	2.0			−2.4	IAA12	Auxin signaling
VIT_05s0094g01010	3.4			−3.3	Indole-3-acetate β-glucosyltransferase	Auxin metabolism
VIT_19s0014g04690	3.6				Indole-3-acetic acid-amido synthetase	Auxin metabolism
VIT_11s0052g00440	29.6			−33.2	PIN1 auxin transport protein	Auxin transport
VIT_04s0008g02800	−17.0		12.5	241.7	SAUR_D	Auxin signaling
VIT_04s0008g06350	59.2				TPR1 (topless-related 1)	Auxin signaling

Table 1. Continued

Gene ID	Fold-change				Functional annotation	Functional category
	EL33 (PM vs control)	EL35 (PM vs control)	Control (EL35 vs EL33)	PM infected (EL35 vs EL33)		
Abscisic acid (ABA)						
VIT_02s0087g00910	2.1				9-*cis*-Epoxycarotenoid dioxygenase	ABA biosynthesis
VIT_01s0026g02190		2.6			ABA-responsive protein (HVA22c)	ABA signaling
VIT_06s0080g00340	129.3			−11.5	ABI5 (ABA insensitive 5)	ABA signaling
VIT_07s0005g05400	22.7				Abscisic acid-insensitive protein 3 (ABI3)	ABA signaling
VIT_14s0006g03250	8.5				AWPM-19	ABA signaling

Complete dataset in Supplementary Table S5.

Regarding auxins, the *Topless-related 1* (*TPR1*) gene, involved in gene repression, was up-regulated in green infected berries, as well as genes coding for auxin transporters, namely *PIN1* and *AUX1*, auxin-responsive proteins and genes involved in auxin metabolism (Table 1; Supplementary Table S5). IAA-amido synthetases are involved in auxin homeostasis through amino acid conjugation (Wang and Fu, 2011). Two *SAUR* genes were down-regulated in response to PM at the green stage (Table 1; Supplementary Table S5). SA-mediated plant immunity was found to up-regulate certain IAA-amido synthase genes and down-regulate *SAUR* genes, as well as genes from the Aux/IAA family (Wang *et al.*, 2007).

Relative to ABA biosynthesis and signaling, genes encoding 9-*cis*-epoxycarotenoid dioxygenase, ABA insensitive, AWPM-19-like proteins, ABA-responsive protein (HVA22c), and protein phosphatase AHG1 were up-regulated in infected berries mostly at the EL33 stage (Table 1; Supplementary Table S5).

Fungal metabolic program during infection putatively involves secretion of effectors and carbohydrate-active enzymes

Raw data from RNA-seq was also aligned with the *E. necator* C-strain genome (Jones *et al.*, 2014) with 5089 (78.5%) of the predicted transcripts detected across infected berries: 4945 at EL33 and 4040 at EL35 (Supplementary Table S7). Several transcripts were detected only in one stage; however, when detected at both developmental stages, no differential expression was observed (Supplementary Table S7).

Effectors are secreted by plant pathogens during infection (Ma and Guttman, 2008). Several putative effector genes were expressed at both developmental stages, including those coding for glucose-repressible alcohol dehydrogenase transcriptional effectors, ribonuclease-like proteins, metallopeptidase RxLR effector, and candidates for secreted effector proteins (CSEPs); nevertheless, the majority of the effectors homologous to *Avrk1* and *Avra10* (EKA)-like protein transcripts were detected at EL33 (Table 2; Supplementary Table S7). Putative effector transcripts were also detected in leaves infected with PM (Jones *et al.*, 2014).

Moreover, several genes encoding fungal carbohydrate-active enzymes (CAZymes), were detected in infected berries at both green and véraison stages, including genes coding for carbohydrate esterase, glycosyltransferases, glycoside hydrolases, and carbohydrate-binding modules (Table 2; Supplementary Table S7).

Moreover, genes involved in chitin biosynthesis, carbohydrate uptake and metabolism, lipid and fatty acid metabolism and transport, nitrogen uptake, and cutin degradation (cutinase) were also expressed at both developmental stages (Table 2; Supplementary Table S7). Expression of genes related to amino acid and polyamine metabolism was also detected. Polyamines have been involved in spore germination, appressorium formation and conidiation (Rocha and Wilson, 2019).

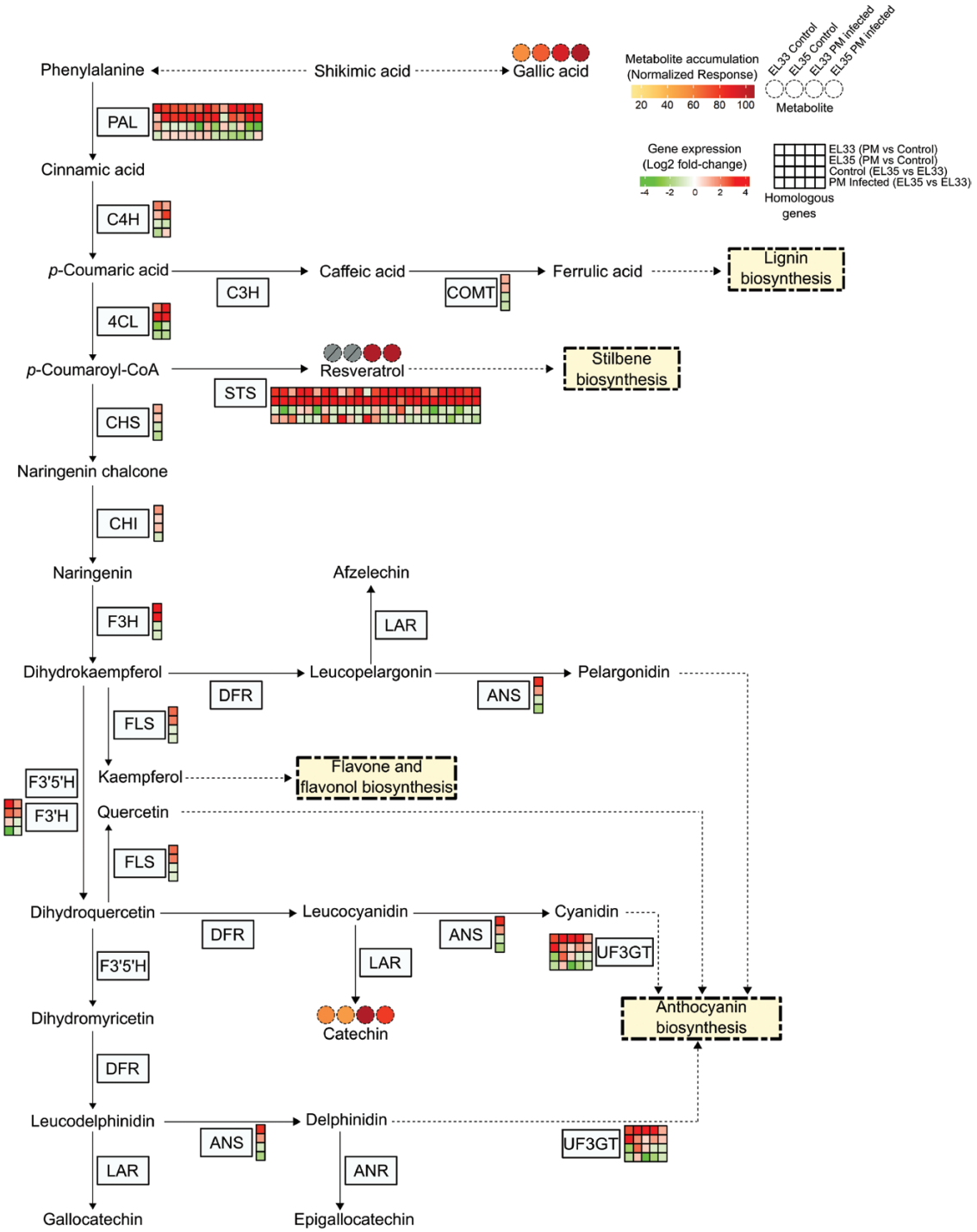

Fig. 6. Activation of phenylpropanoid metabolism in response to powdery mildew (PM) infection. Phenylpropanoid and flavonoid pathway representation based on KEGG pathways (www.genome.jp/kegg/pathway.html). Dashed lines represent omitted steps. Heatmap colors represent the gene expression ($\log_2$ fold change) for each comparison (Supplementary Table S5). Circles represent metabolites and colors the normalized response in each condition (Supplementary Table S4). Crossed grey circles represent non-detected metabolites. EL33, green stage; EL35, véraison stage. 4CL, 4-coumaroyl-CoA ligase; ANR, anthocyanidin reductase; ANS, anthocyanidin synthase; C3H, *p*-coumarate 3-hydroxylase; C4H, *trans*-cinnamate 4-monooxygenase; CHI, chalcone isomerase; CHS, chalcone synthase; COMT, caffeic acid 3-*O*-methyltransferase; DFR, dihydroflavanol 4-reductase; F3H, flavonone 3-hydroxylase; F3′H, flavonoid 3′-monooxygenase; F3′5′H, flavonoid 3′,5′-hydroxylase; FLS, flavonol synthase; LAR, leucoanthocyanidin reductase; PAL, phenylalanine ammonia-lyase; STS, stilbene synthase; UF3GT, UDP-glucose:anthocyanidin 3-*O*-D-glucosyltransferase.

Table 2. Selection of *Erysiphe necator* genes in powdery mildew-infected grape berries

Transcript ID	Functional annotation	Present at EL33	Present at EL35
Effectors			
EV44_t0562	celp0028 effector like protein	+	+
EV44_t0361	csep0049 effector protein	+	+
EV44_t0037	csep0242 effector protein	+	
EV44_t0277	EKA-like protein	+	
EV44_t2445	EKA-like protein	+	
EV44_t5321	Glucose-repressible alcohol dehydrogenase transcriptional effector	+	+
EV44_t5307	Metallopeptidase RXLR effector	+	+
EV44_t2234	RNA binding effector protein Scp160	+	+
EV44_t4585	Secreted effector protein	+	+
EV44_t5361	Secreted effector protein	+	
EV44_t4200	Virulence effector		+
CAZymes and cell wall metabolism			
EV44_t0515	Carbohydrate esterase family 5 protein	+	+
EV44_t2590	Carbohydrate-binding module family 48 protein	+	+
EV44_t3003	Cell wall glucanase	+	+
EV44_t2782	Chitin deacetylase	+	+
EV44_t4424	Chitin synthase	+	+
EV44_t1121	Dolichyl glycosyltransferase	+	+
EV44_t0156	Endo-β-glucanase	+	+
EV44_t4885	Glucan synthesis regulatory protein	+	+
EV44_t0185	Glucan-β-glucosidase	+	+
EV44_t0299	Glycoside hydrolase	+	+
EV44_t0133	Glycoside hydrolase deacetylase	+	+
EV44_t0070	Glycosyltransferase family protein	+	
EV44_t0089	GPI-anchored cell wall β-endoglucanase	+	+
Carbohydrate metabolism			
EV44_t0308	Fumarate reductase	+	+
EV44_t1203	High-affinity glucose transporter	+	+
EV44_t0140	Malate dehydrogenase	+	+
EV44_t2476	Maltose permease	+	+
EV44_t6497	*myo*-Inositol transporter	+	
EV44_t2456	Raffinose synthase SIP1	+	+
EV44_t0175	Sucrose transporter	+	+
EV44_t6132	Sugar transporter	+	+
EV44_t2035	UDP-galactose transporter like protein	+	+
Fatty acid metabolism			
EV44_t0455	1-Acyl-*sn*-glycerol-3-phosphate acyltransferase γ	+	+
EV44_t0138	Extracellular lipase	+	+
EV44_t4768	Fatty acid desaturase	+	+
EV44_t5564	Fatty acid elongase	+	+
EV44_t2281	Fatty acid hydroxylase	+	+
EV44_t1141	Fatty acid oxygenase	+	+
EV44_t2517	Fatty acid synthase subunit alpha	+	+
EV44_t0030	Fatty acid transporter	+	+
EV44_t5122	Lipase	+	+
EV44_t5957	Omega-3 fatty acid desaturase	+	+
EV44_t2799	Phospholipase D1	+	+
EV44_t0377	Triacylglycerol lipase	+	+
Nitrogen metabolism			
EV44_t5850	Ammonium transporter	+	+
EV44_t1219	Nitrate reductase	+	+
EV44_t2316	Nitrilase family protein	+	+
EV44_t5397	Nitrogen response regulator	+	+

Table 2. Continued

Transcript ID	Functional annotation	Present at EL33	Present at EL35
Cutin			
EV44_t0350	Cutinase	+	+
Amino acid and polyamine metabolism			
EV44_t2279	Argininosuccinate lyase	+	+
EV44_t0887	Argininosuccinate synthetase	+	+
EV44_t2411	Asparagine synthetase	+	+
EV44_t1489	Glutamine synthetase	+	+
EV44_t1419	Ornithine carbamoyltransferase	+	+
EV44_t2871	Ornithine decarboxylase	+	
DNA modification and chromatin remodeling			
EV44_t4654	DNA helicase	+	+
EV44_t1446	Histone acetyltransferase esa1	+	+
EV44_t4537	Histone chaperone	+	+
EV44_t1305	Histone deacetylase	+	+
EV44_t1301	Histone lysine methyltransferase set7 protein	+	
EV44_t5676	Histone promoter control 2 protein	+	+
EV44_t1760	Histone-arginine methyltransferase carm1	+	+
EV44_t5518	Histone-fold containing protein	+	+
DNA replication, cytoskeleton remodeling and cell cycle			
EV44_t1692	Actin cytoskeleton organization protein	+	+
EV44_t0739	40S ribosomal protein s24	+	+
EV44_t0756	60S ribosomal protein l38	+	+
EV44_t1816	Cell cycle control protein	+	+
EV44_t1527	Cell cycle control protein cwf14	+	+
EV44_t0423	Cell cycle checkpoint protein	+	+
EV44_t2724	Anaphase-promoting complex protein	+	
EV44_t4904	Anaphase promoting complex subunit protein	+	+

Complete dataset in Supplementary Table S7.

Genes related to DNA modification and chromatin remodeling, including histones, helicases, and histone acetyltransferases, deacetylases, and demethylases, were also expressed during infection (Table 2; Supplementary Table S7) and may suggest epigenetic regulation of pathogenic traits (Gómez-Díaz *et al.*, 2012). Chromatin-based control mechanisms have been shown to regulate effector gene expression of plant-associated fungi (Soyer *et al.*, 2015). Additionally, also noteworthy was the expression of genes involved in DNA replication, cytoskeleton remodeling and cell cycle, such as those coding for actin cytoskeleton organization proteins, ribosomal proteins, cell cycle control, checkpoint proteins, and anaphase-promoting complex, which indicates proliferation of the fungus.

Phytohormonal analysis indicates the involvement of salicylic acid and jasmonates in response to powdery mildew

Phytohormonal analysis revealed that PM infection caused an accumulation of SA and SA-β-D-glucoside at both stages, though more pronounced at EL33 (Fig. 7). Moreover, GC-TOF-MS analysis also identified the SA-β-D-glucoside (salicylic acid-glucopyranoside), a SA sugar conjugate, as a marker of infection at the green stage (Fig. 4). SA is widely associated with the defense response to biotrophic fungi (reviewed by Glazebrook, 2005).

Relative to jasmonates, content of JA and its precursor 12-oxo-phytodienoic acid (*cis*-OPDA) was not affected by infection (Fig. 7). However, 12-*O*-glucoside-JA was accumulated in infected berries at both stages with higher levels at the green stage (Fig. 7), suggesting activation of JA glycosylation in response to PM infection. JA-Ile and OH-JA-Ile showed a tendency to increase in response to PM; however, no differences were observed for dicarboxyjasmonoyl-isoleucine (COOH-JA-Ile) (Fig. 7).

Overall, the results not only reinforce the involvement of SA as regulator of defense against *E. necator*, but also suggest a reprogramming of the jasmonate pathway. Additionally, the results showed no significant alteration in the content of IAA and ABA in response to PM (Fig. 7).

Global changes in the transcriptome and metabolome of ripening berries induced by the fungus

The main ripening parameters were not significantly affected by PM infection except for anthocyanin accumulation, which seems to be anticipated in infected green fruits

(Fig. 2). Nevertheless, only 31.2% of the genes exhibited the same trend in expression when comparing control (EL35 versus EL33) and infected berries (EL35 versus EL33) indicating an impact in the onset of ripening caused by the infection.

Transcription factors and hormones are key regulators of berry development and ripening (Fortes *et al.*, 2011, 2015). In this study, several transcription factor families were differentially modulated in infected compared with control berries (Supplementary Fig. S7; Supplementary Tables S5, S8). On the other hand, ethylene- and auxin-mediated signaling, were functional categories enriched only in PM-infected berries (Supplementary Fig. S7; Supplementary Table S6).

Powdery mildew infection seemed also to affect the primary and secondary metabolisms of ripening berries. The carbohydrate metabolism was a functional category enriched

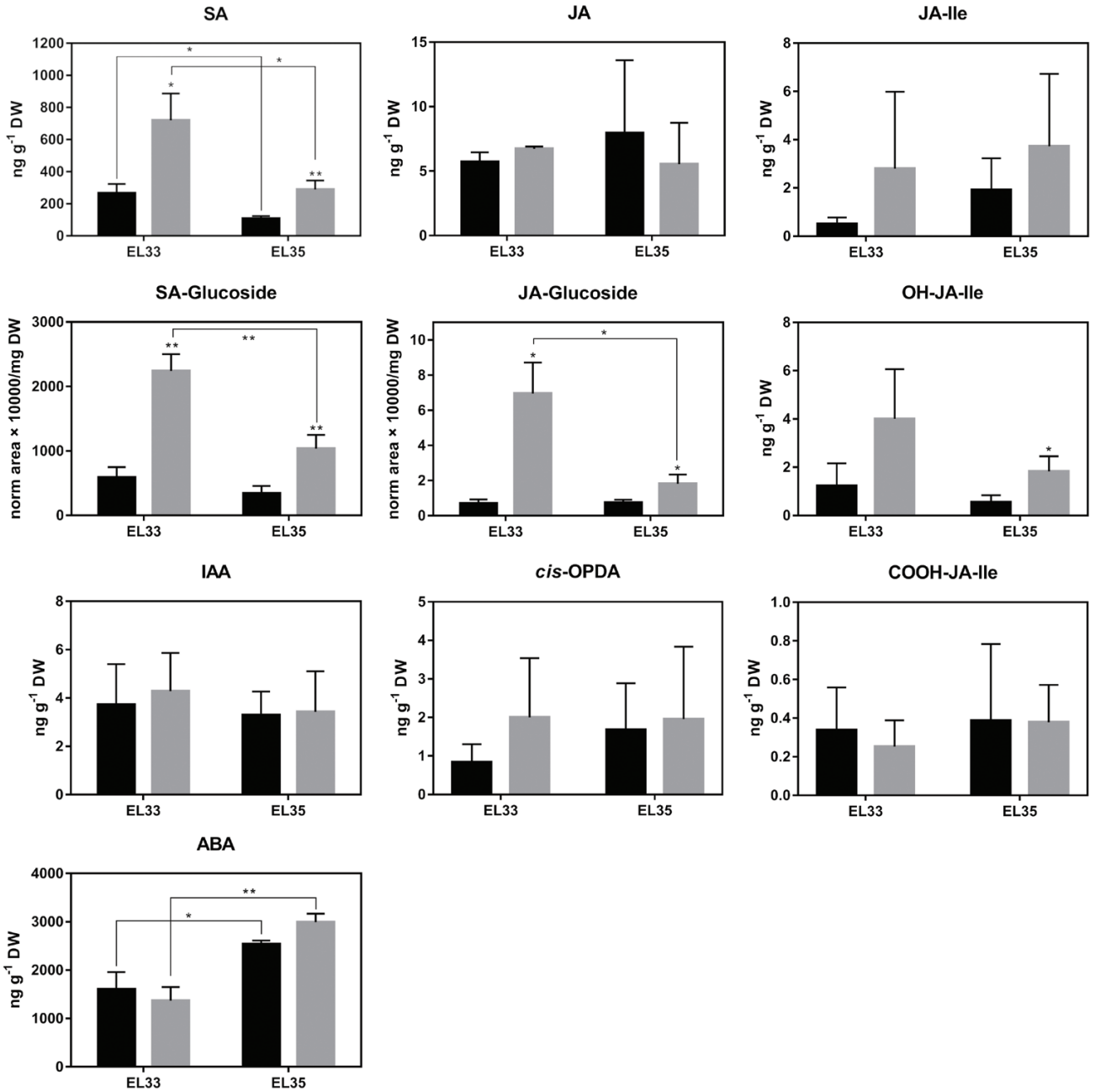

Fig. 7. Hormonal profiling of powdery mildew (PM)-infected and control grape berries at green (EL33) and véraison (EL35) stages. Bars and whiskers represent means and standard deviation (SD). Asterisks indicate statistical significance on pairwise comparisons (Student's *t*-test: **P*≤0.05, ***P*≤0.01). ABA, abscisic acid; COOH-JA-Ile, dicarboxyjasmonoyl-isoleucine; *cis*-OPDA, 12-oxo-phytodienoic acid; IAA, indole acetic acid; JA, jasmonic acid; JA-glucoside, 12-*O*-glucoside jasmonic acid; JA-Ile, conjugate jasmonoyl isoleucine; OH-JA-Ile, hydroxyjasmonoyl-isoleucine; SA, salicylic acid; SA-glucoside, salicylic acid-β-D-glucoside.

as up-regulated and photosynthesis enriched as down-regulated only in the PM-infected berries (Supplementary Fig. S7; Supplementary Tables S5, S6, S8). Reprogramming of cell wall metabolism was also affected by the presence of the fungus in the berry (Supplementary Tables S5, S8). Genes involved in fatty acid metabolism were modulated differently in the presence of the fungus whereas the accumulation of hexacosanoic, octacosanoic, and pentacosanoic acids was anticipated in infected berries at the green stage (Fig. 3). Interestingly, phenylpropanoid metabolism and flavonoid biosynthesis were véraison-response categories enriched in control berries as up-regulated and in infected berries as down-regulated (Supplementary Fig. S7; Supplementary Table S6). In accordance, the levels of epigallocatechin decreased during ripening only in infected berries (Fig. 3).

Taken together, the results showed that powdery mildew infection impacted regulation of ripening and parameters involved in fruit quality.

Discussion

Powdery mildew is one of the most widespread diseases of *V. vinifera* plants (Fig. 1). It is caused by the obligate biotrophic fungus *E. necator*, which depends on the host cells to complete its life cycle. Most of the studies performed so far have focused on leaves and revealed that susceptible grapevines widely activate genes associated with defense (Fung *et al.*, 2008; Fekete *et al.*, 2009; Toth *et al.*, 2016). Nevertheless, understanding how fruits respond to these biotrophic fungal pathogens is essential for grapevine improvement, since some responses can be organ specific. In fact, the isoprenoid biosynthetic pathway was reported to be responsive to *E. necator* infection in leaves (Fung *et al.*, 2008; Toth *et al.*, 2016), whereas this was not observed in this study, though it should be considered that different cultivars were analysed. Additionally, omics data revealed an accumulation of long-chain fatty acids in infected berries (Fig. 3), whereas transcriptional profiling of infected leaves suggested activation of fatty acid degradation pathways (Fung *et al.*, 2008).

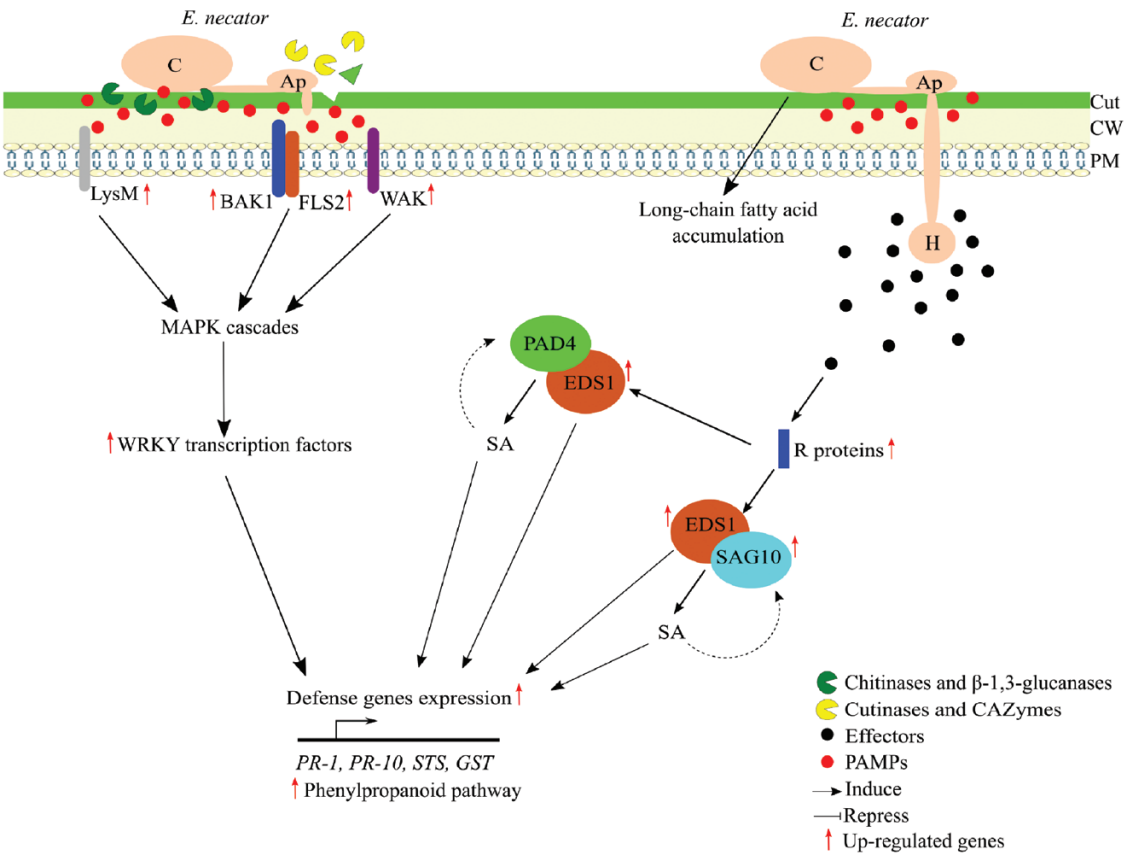

Fig. 8. Overview of defense responses during *Erysiphe necator* infection in grape berries. During powdery mildew infection, pattern recognition receptors (PRRs) recognize pathogen-associated molecular patterns (PAMPs) initiating PAMP-triggered immunity (PTI): MAPK cascades are activated acting on WRKY transcription factors that, in turn, regulate the expression of defense-associated genes. Host cells release chitinases and β-1,3-glucanases that act on the fungal cell wall releasing chitin that is perceived by PRRs such as LysM receptor like-kinases. To suppress PTI, the fungus releases effectors that are then sensed by R proteins in the cytoplasm, activating the ETI. This activation is facilitated by EDS1–PAD4 and EDS1–SAG101 complexes. Salicylic acid has a central role in defense against powdery mildew. *E. necator* infection also leads to the accumulation of long-chain fatty acids. Ap, appressorium; C, conidia; Cut, cutin; CW, cell wall; H, haustorium; PM, plasma membrane.

The combination of multiple omics may provide evidence on berry defense mechanisms and ontogenetic resistance. In this study, it was shown that defensive strategies were more active at the green stage (Fig. 5), which might be related to the fact that *E. necator* usually infects photosynthetic tissues. Ontogenetic resistance has been observed in susceptible berries and in older leaves in the transition from source to sink (Gadoury *et al.*, 2003; Ficke *et al.*, 2003; Calonnec *et al.*, 2018). However, this timing may also depend on the susceptibility of the variety. In the extremely susceptible 'Carignan', EL35 samples with 25–30% colored berries are not yet resistant and it is likely that this resistance will appear at full véraison when chlorophyll-containing tissue is no longer present.

Powdery mildew infection generates plant immunity-related responses in susceptible grape berries

Transcriptomic data revealed an activation of defense responses (Fig. 8) in susceptible grape berries. Pathogen infection is known to trigger innate immunity through PTI, i.e., through the recognition of PAMPs by extracellular pattern-recognition receptors (PRRs) located at the plasma membrane of the host cells (Jones and Dangl, 2006). Several PRR-encoding genes were activated in infected berries at both stages, including *BAK1*, *FLS2*, and *WAK*. Moreover, several other genes coding for kinase receptors, including leucine-rich repeat receptor kinases (LRR-RKs) and Ser/Thr receptor-like kinases, were up-regulated upon infection, indicating an activation of PTI. BAK1 is a leucine-rich repeat receptor-like protein kinase that forms a complex with FLS2 and with other LRR-RKs after ligand perception, activating downstream signaling responses (Schulze *et al.*, 2010; Roux *et al.*, 2011). WAKs are receptor-like kinases that recognize both pectins from the cell wall and pectin fragments, oligogalacturonic acids (OGs), derived from pathogen action, activating defense responses through MAPK cascades (Kohorn and Kohorn, 2012). *Clavata1 receptor kinase* (*CLV1*) genes were also up-regulated in response to PM infection but were down-regulated in berries infected with *Botrytis cinerea* (Agudelo-Romero *et al.*, 2015), indicating different responses of grape tissues to biotrophs and necrotrophs.

Chitin, which is found in fungal cell walls, is perceived through plant LysM receptor like-kinases (LysM-RKs) initiating defense responses (Wan *et al.*, 2008). One chitin elicitor-binding protein containing a LysM motif was responsive to PM berry infection at the véraison stage. *V. vinifera* LysM-RKs were shown to be involved in chitooligosaccharide-triggered immunity and in penetration resistance to *E. necator* (Brulé *et al.*, 2019). During infection, fungal pathogens can release hydrolytic enzymes that target the plant cuticle such as cutinases, esterases, and lipases. In fact, cuticle is an important barrier against fungal infection (Ziv *et al.*, 2018). Enzymes that target the cell wall such as CAZymes also facilitate fungal penetration (Cantarel *et al.*, 2009). Several CAZyme genes were expressed in PM-infected leaves (Jones *et al.*, 2014). In this study, *E. necator* transcripts coding for these hydrolytic enzymes were detected along with *V. vinifera* transcripts coding for chitinases and β-1,3-glucanases (Fig. 8), supporting the successful infection of the 'Carignan' grape berries.

Adapted pathogenic species are supposed to release effectors to suppress PTI. In turn, host plants activate a second layer of resistance, ETI, through the recognition of those effectors by R proteins (Jones and Dangl, 2006). Activation of ETI can result in a hypersensitive response at the infection site. In this study, up-regulated genes at both stages were enriched in the NBS-LRR family category involved in PM response (Fig. 5; Goyal *et al.*, 2020). Activation of ETI in susceptible leaves under infection with PM has been previously reported though this activation may be delayed or with a level of up-regulation of related genes lower than in resistant or partially resistant plants (Gao *et al.* 2010; Amrine *et al.* 2015; Goyal *et al.* 2020) Additionally, several other genes encoding R proteins, including EIX receptors, were up-regulated in infected berries (Table 1). Putative *E. necator* effector transcripts were also detected, including those coding for EKA-like proteins and CSEP (Table 2), which might influence the host plant immunity. Most of the EKA-like protein transcripts were detected only at the green stage, suggesting that they might be associated with an earlier stage of infection.

Upon pathogen sensing and receptor activation, MAPK signaling cascades are initiated and act on WRKY transcription factors, which are regulators of defense responses to several pathogens (Eulgem and Somssich, 2007). WRKY transcription factor family and protein kinases were functional categories significantly enriched in response to PM. Up-regulated *WRKY* genes included *WRKY33* and *WRKY71*, which were shown to be involved in defense in grapevine, Arabidopsis, and rice (Zheng *et al.*, 2006; Liu *et al.*, 2007; Merz *et al.*, 2015). As observed in this work, *WRKY* genes were also induced in PM-infected leaves of susceptible *V. vinifera* cv. Cabernet Sauvignon (Fung *et al.*, 2008), and its ectopic expression was shown to increase resistance to PM (Li *et al.*, 2010; Zhu *et al.*, 2012; Wang *et al.*, 2017).

Overall, data indicate that susceptible berries were able to activate defenses in response to *E. necator* (Fig. 8). This was also observed on 'Cabernet Sauvignon' leaves, suggesting that PM-susceptible plants are able to initiate basal defenses in different organs; however, responses are not enough to restrict fungal growth or to mitigate disease progression (Fung *et al.*, 2008; Fekete *et al.*, 2009). Activated defense in leaves was also shown to include the expression of *EDS1*, *MAPKK*, *WRKY*, *PR-1*, *PR-10*, and *STS* (Fung *et al.*, 2008), though the expression of different paralogous genes was often observed when comparing berries and leaves from the varieties 'Carignan' and 'Cabernet Sauvignon', respectively.

Despite the induction of defensive strategies, 'Carignan' berries were susceptible to infection, which could be due to overexpression of *MLO* genes (Table 1). MLO proteins are known to be essential in the successful penetration of adapted

PM species on several host plants (Kusch and Panstruga, 2017). *VvMLO3*, *VvMLO4*, and *VvMLO17* were shown to be up-regulated upon *E. necator* inoculation in 'Cabernet Sauvignon' leaves and may act as *S*-genes (Feechan *et al.*, 2008). Moreover, knockdown of *VvMLO7* and *VvMLO6* resulted in reduced PM severity (Pessina *et al.*, 2016). Results suggest that 'Carignan' susceptibility to PM could be due, at least partially, to increased expression of *S*-genes. The presence of *S*-genes in *V. vinifera* was observed in 'Chardonnay', in which the QTL *Susceptibility to Erysiphe necator 1* (*Sen1*) was identified as a source of susceptibility (Barba *et al.*, 2014).

Response to powdery mildew infection is putatively regulated by the interaction of salicylic and jasmonic acid metabolism

Hormonal metabolism was strongly reprogrammed in response to PM infection (Fig. 7; Table 1). SA is known to be a key regulator of response to infection by biotrophic fungi, including powdery mildew (Fung *et al.*, 2008), by modulating the expression of several defense-related genes. Hormonal quantification revealed that free and conjugated SA levels increased in PM-infected berries, as observed in susceptible 'Cabernet Sauvignon' PM-infected leaves (Fung *et al.*, 2008). EDS1 is a key regulator of innate immune responses against pathogens infection and interacts with two signaling partners, phytoalexin-deficient 4 (PAD4) and senescence-associated gene 101 (SAG101), regulating the SA signaling pathway in Arabidopsis (Feys *et al.*, 2005; Wagner *et al.*, 2013). In this study, both *EDS1* and *SAG101* homologous genes were up-regulated in response to infection (Fig. 8). Previous studies showed that *EDS1* promoter is induced by SA and *EDS1* levels in resistant *V. aestivalis* leaves were constitutively higher compared with the susceptible 'Cabernet Sauvignon', where infection induced *EDS1* expression (Fung *et al.*, 2008; Gao *et al.*, 2010, 2014). In Arabidopsis, an EDS1–PAD4 complex was found to be essential in basal resistance (Rietz *et al.*, 2011). However, the expression of the grape *PAD4* homologous gene was not affected by PM infection in leaves (Fung *et al.*, 2008). The role of EDS1–PAD4 grape homologs might be more complex than in Arabidopsis (Gao *et al.*, 2014), and post-transcriptional regulation could ultimately be responsible for PAD4 activation. Some of the defense-related genes activated in infected grape berries, including *PR-1* genes and genes for β-1,3-glucanase and glutaredoxin, were previously shown to be responsive not only to PM infection but also to SA treatment in leaves (Toth *et al.*, 2016). Nevertheless, during ETI, SA-responsive genes were proposed to be regulated by SA-independent mechanisms as well, increasing the robustness of the innate immunity (Tsuda *et al.*, 2013).

JA signaling is classically associated with responses against necrotrophic pathogens. In this study, activation of genes related to JA biosynthesis (*VviLOX* and *VviAOS*) was not corroborated by increased contents of *cis*-OPDA and JA (Fig. 7). Up-regulation of these genes was also observed in 'Cabernet Sauvignon' leaves infected with PM (Toth *et al.*, 2016). On the other hand, JA-glucoside was highly accumulated in infected berries possibly due to a redirection of JA to its conjugated form. Moreover, a tendency to increase in response to PM was observed for JA-Ile and 12-OH-JA-Ile. JA-Ile is the most bioactive jasmonate (Staswick and Tiryaki, 2004), and hydroxylation leads to its catabolic inactivation (Koo *et al.*, 2011, 2014). However, Jimenez-Aleman and co-workers (2019) demonstrated that 12-OH-JA-Ile might regulate specific jasmonate-dependent responses. Nevertheless, the accumulation of JA-glucoside suggests that the inactivation of jasmonates is initiated rather than the activation of JA-dependent pathways. The specific activity of JA-glucoside has not been described in the context of defense (Nakamura *et al.*, 2011). Additionally, the involvement of JA signaling in biotroph infection is still poorly understood. The JA signaling pathway was shown to be activated in cells surrounding the central SA-active cells around the infection sites during ETI in Arabidopsis (Betsuyaku *et al.*, 2018). Thus, a detailed spatial analysis of jasmonates and SA together with metabolic flux analysis of the jasmonate pathway could confirm a modulation of jasmonate metabolism in response to PM. Recent studies confirmed that the samples used in this study were infected only with PM (Brás et al., 2021). Additionally, exogenous application of methyl jasmonate on *V. vinifera* plants elicited tolerance to *E. necator* infection and JA signaling was associated with defense responses against PM in grapevine (Belhadj *et al.*, 2006). Thus, we cannot exclude that jasmonates might function in the SA-mediated responses in a crosstalk manner (Robert-Seilaniantz *et al.*, 2011) and possibly in interaction with signaling pathways involving ABA and IAA (Coelho *et al.*, 2019).

Erysiphe necator *induced the reprogramming of berry metabolism and altered specific ripening processes*

Transcriptional and metabolic data suggested a reprogramming of several plant metabolic pathways in response to *E. necator* (Figs 3, 5).

At the first stage of infection the pathogen faces the protective plant cuticle (Ziv *et al.*, 2018, Lara *et al.*, 2019). Data suggest reprogramming of cuticle composition with a putative decrease in specific triterpenoids, important components of fruit cuticular wax (Lara *et al.*, 2015). In addition, an increase was noticed in several long-chain saturated fatty acids (eicosanoic and docosanoic acids; Fig. 4), which are biosynthetic precursors of cutin and wax and the main components of the plant cuticle (Ziv *et al.*, 2018). Three *V. vinifera* genes (*Ethylene-responsive transcription factor ERF003*, *Eceriferum 2-CER2*, *Cuticle protein*) involved in the cuticular wax biosynthetic pathway (Dimopoulos *et al.*, 2020) were also modulated due to the infection highlighting the importance of this structural defense. Powdery mildew was previously reported to modify the fatty acid profile of fully developed infected

berries and to induce the synthesis of eicosanoic acid (Petrovic *et al.*, 2017). Several fatty acids from leaf and/or berry cuticular waxes of resistant genotypes were shown to have antifungal activity (Özer *et al.*, 2017). Accumulation of long-chain fatty acids, as well as up-regulation of genes coding for acyl-CoA synthases, was also observed in 'Trincadeira' berries infected with *B. cinerea* (Agudelo-Romero *et al.*, 2015), suggesting a role in response to not only biotrophic but also necrotrophic fungi (Commenil *et al.*, 1997). However, fatty acid biosynthesis was reported to be down-regulated in response to PM in leaves together with an up-regulation of genes related to fatty acid degradation (Fung *et al.*, 2008), suggesting that fatty acid modulation might be organ-specific. Eventually, accumulation of fatty acids in berries could constitute an energy source for the fungus that activates its transport and metabolism.

Nitrogen (N) metabolism was one of the functional categories enriched in up-regulated infection-responsive genes including those coding for nitrate and ammonium transporters. Pike and co-workers (2014) observed an up-regulation upon PM infection of the nitrate transporter gene *VvNPF3.2* in susceptible 'Cabernet Sauvignon' grapevine and *AtNPF3.1* in Arabidopsis, suggesting that the pathogen influences host metabolism to increase nitrate transport. Nitrogen is essential for fungal growth and Jones and co-workers (2014) demonstrated that *E. necator* lacks some genes involved in nitrate metabolism, which might be associated with the obligate biotrophic lifestyle, supporting the observed activation of host and pathogen genes related to N transport.

Genes encoding sugar and polyol transporters, as well as genes related to sugar metabolism, were up-regulated in response to PM infection in Arabidopsis (Fotopoulos *et al.*, 2003). Hexose transporter genes were also up-regulated in grape leaves upon *E. necator* infection (Hayes *et al.*, 2010). On the other hand, the fungal transcriptome included several transcripts involved in carbohydrate uptake and metabolism, indicating that reprogramming of sugar metabolism in grapes is at least partially directed towards fungal consumption. These sugars may also be used as precursors of plant secondary metabolites. Gallic acid and stigmasterol were among the putative markers of infection with antifungal properties (Lattanzio *et al.*, 2006) and/or known roles in plant–pathogen interactions (Griebel and Zeier, 2010). Powdery mildew infection induced the activation of phenylpropanoid pathway genes and accumulation of catechins, resveratrol, and anthocyanins (Fig. 6). Additionally, infection seems to deregulate the normal course of the phenylpropanoid pathway during grape ripening (Supplementary Table S8).

Conclusions

This work integrates for the first time the transcriptional, metabolic, and hormonal profiling of 'Carignan' grape berries infected with PM. PM-susceptible grape berries were able to induce defensive mechanisms, but these responses were not enough to restrict fungal infection, eventually due to a delayed activation. Validation of post-infection defensive responses identified in this study in susceptible fruits of other varieties together with confirmation of pre-infection defensive responses in resistant fruits will provide valuable information in the context of grapevine improvement. Alternatively, grapevine susceptibility genes or fungal virulence genes, namely those favoring fungal growth and pathogenesis, may be subjected to gene editing once validated.

Specific responses, namely the reprogramming of fatty acid metabolism and isoprenoid biosynthesis, together with putative alterations in structural components of cuticle, were different in grape berries compared with what was previously reported in leaves, highlighting the importance of studying fungal responses in different grapevine organs. Results also suggest an involvement of jasmonate metabolism against PM. These hormones are not classically associated with response to biotrophic fungi, in contrast to the known role of SA. Moreover, this study indicated how both fruit and fungal metabolism was reprogrammed under infection and how it induced deregulation of early stages of berry ripening. Additionally, several metabolites, such as resveratrol, gallic acid, eicosan-1-ol, eicosanoic, and docosanoic acids, can be further validated for ulterior use as markers of infection at early ripening stages under field conditions.

Supplementary data

Supplementary data are available at JXB online.

Fig. S1. *Erysiphe necator* biomass accumulation in powdery mildew infected and control grape berries at green and véraison stages.

Fig. S2. Principal component analysis of metabolic profiles of infected and control grape berries at two ripening stages.

Fig. S3. Venn diagrams of differentially expressed genes in response to infection and ripening.

Fig. S4. Multidimensional scaling of RNAseq analysis of infected and control grape berries at two ripening stages.

Fig. S5. Real-time PCR validation of gene expression.

Fig. S6. Pearson correlation between gene expression data obtained with real-time PCR and RNA-seq data.

Fig. S7. Enriched functional subcategories in RNAseq data.

Fig. S8. Total phenolic content and phenylalanine ammonia-lyase enzyme assay.

Table S1. List of primers used in real-time PCR.

Table S2. Summary of RNA-seq sequencing and mapping statistics.

Table S3. Details of phytohormones´ analysis by LC-MS/MS in negative ionization mode.

Table S4. Normalized responses of profiled volatile and polar metabolites from control and infected berries.

Table S5. List of *Vitis vinifera* differentially expressed genes.

Table S6. Functional enrichment analysis of differentially expressed genes in response (A) to PM infection and (B) to véraison stage.

Table S7. List of *Erysiphe necator* predicted genes in infected berries at green (EL33) and véraison (EL35) stages.

Table S8. Selection of véraison-responsive genes in powdery mildew (PM) infected and control grape berries.

Acknowledgements

We thank Ines Fehrle, Max-Planck-Institut für Molekulare Pflanzenphysiologie, 14476 Potsdam-Golm, Germany, for her technical support of the GC-EI/TOF-MS and GC-EI/QUAD-MS measurements. We also thank Dr Michael Reichelt and Andrea Lehr, MPI for Chemical Ecology for technical support in phytohormone analysis, and Jose Saramago Natividade (BASF, Portugal) for his support in collecting samples from the field. This work was supported by UIDB/04046/2020 and UIDP/04046/2020 Centre grants from FCT, Portugal (to BioISI). DP and FS are recipients of fellowships from BioSys PhD program PD65-2012 (Refs PD/BD/114385/2016 and PB/BD/130976/2017) from FCT (Portugal). This work was supported by Fundação para a Ciência e Tecnologia-funded research project "GrapInfectomics" (PTDC/ASP-HOR/28485/2017). Additionally, it was partially supported by the Spanish Ministry of Economy project BIO2017-86375-R. This article/publication is based upon work from COST Action CA 17111 INTEGRAPE, supported by COST (European Cooperation in Science and Technology).

Author contributions

AMF: conceptualization; DP, CR, and AMF: sample collection; DP, RA, and FS: nucleic acid extractions, real-time PCR and the biochemical assays; DP and AE: metabolomic analysis; DP and NM: transcriptomic analysis. AM: hormonal profiling. DP: writing -original draft; JK, AM, and JMMZ and AMF: writing – review & editing; AMF and JK: supervision.

Data availability

All data supporting the findings of this study are available within the paper and within its supplementary data published online. RNA-seq data are available at the NCBI SRA database under accession number PRJNA613636.

References

Agudelo-Romero P, Erban A, Rego C, Carbonell-Bejerano P, Nascimento T, Sousa L, Martínez-Zapater JM, Kopka J, Fortes AM. 2015. Transcriptome and metabolome reprogramming in *Vitis vinifera* cv. Trincadeira berries upon infection with *Botrytis cinerea*. Journal of Experimental Botany **66**, 1769–1785.

Agudelo-Romero P, Erban A, Sousa L, Pais MS, Kopka J, Fortes AM. 2013. Search for transcriptional and metabolic markers of grape pre-ripening and ripening and insights into specific aroma development in three Portuguese cultivars. PLoS One **8**, e60422.

Al-Shahrour F, Minguez P, Tárraga J, Medina I, Alloza E, Montaner D, Dopazo J. 2007. FatiGO +: a functional profiling tool for genomic data. Integration of functional annotation, regulatory motifs and interaction data with microarray experiments. Nucleic Acids Research **35**, W91–W96.

Amrine KC, Blanco-Ulate B, Riaz S, Pap D, Jones L, Figueroa-Balderas R, Walker MA, Cantu D. 2015. Comparative transcriptomics of central Asian *Vitis vinifera* accessions reveals distinct defense strategies against powdery mildew. Horticulture Research **2**, 15037.

Anders S, Pyl PT, Huber W. 2015. HTSeq—a Python framework to work with high-throughput sequencing data. Bioinformatics **31**, 166–169.

Barba P, Cadle-Davidson L, Harriman J, Glaubitz JC, Brooks S, Hyma K, Reisch B. 2014. Grapevine powdery mildew resistance and susceptibility loci identified on a high-resolution SNP map. Theoretical and Applied Genetics **127**, 73–84.

Belhadj A, Saigne C, Telef N, Cluzet S, Bouscaut J, Corio-Costet MF, Mérillon JM. 2006. Methyl jasmonate induces defense responses in grapevine and triggers protection against *Erysiphe necator*. Journal of Agricultural and Food Chemistry **54**, 9119–9125.

Belhadj A, Telef N, Cluzet S, Bouscaut J, Corio-Costet MF, Mérillon JM. 2008. Ethephon elicits protection against *Erysiphe necator* in grapevine. Journal of Agricultural and Food Chemistry **56**, 5781–5787.

Betsuyaku S, Katou S, Takebayashi Y, Sakakibara H, Nomura N, Fukuda H. 2018. Salicylic acid and jasmonic acid pathways are activated in spatially different domains around the infection site during effector-triggered immunity in *Arabidopsis thaliana*. Plant & Cell Physiology **59**, 8–16.

Bradford MM. 1976. A rapid and sensitive method for the quantitation of microgram quantities of protein utilizing the principle of protein-dye binding. Analytical Biochemistry **72**, 248–254.

Brás EJS, Fortes AM, Esteves T, Chu V, Fernandes P, Conde JP. 2021. Microfluidic device for multiplexed detection of fungal infection biomarkers in grape cultivars. The Analyst **145**, 7973–7984.

Brulé D, Villano C, Davies LJ, *et al.* 2019. The grapevine (*Vitis vinifera*) LysM receptor kinases VvLYK1-1 and VvLYK1-2 mediate chitooligosaccharide-triggered immunity. Plant Biotechnology Journal **17**, 812–825.

Calonnec A, Cartolaro P, Poupot C, Dubourdieu D, Darriet P. 2004. Effects of *Uncinula necator* on the yield and quality of grapes (*Vitis vinifera*) and wine. Plant Pathology **53**, 434–445.

Calonnec A, Jolivet J, Vivin P, Schnee S. 2018. Pathogenicity traits correlate with the susceptible *Vitis vinifera* leaf physiology transition in the biotroph fungus *Erysiphe necator*: an adaptation to plant ontogenic resistance. Frontiers in Plant Science **9**, 1808.

Cantarel BL, Coutinho PM, Rancurel C, Bernard T, Lombard V, Henrissat B. 2009. The Carbohydrate-Active EnZymes database (CAZy): an expert resource for glycogenomics. Nucleic Acids Research **37**, D233–D238.

Coelho J, Almeida-Trapp M, Pimentel D, Soares F, Reis P, Rego C, Mithöfer A, Fortes AM. 2019. The study of hormonal metabolism of Trincadeira and Syrah cultivars indicates new roles of salicylic acid, jasmonates, ABA and IAA during grape ripening and upon infection with *Botrytis cinerea*. Plant Science **283**, 266–277.

Commenil P, Brunet L, Audran J-C. 1997. The development of the grape berry cuticle in relation to susceptibility to bunch rot disease. Journal of Experimental Botany **48**, 1599–1607.

Conde A, Pimentel D, Neves A, Dinis LT, Bernardo S, Correia CM, Gerós H, Moutinho-Pereira J. 2016. Kaolin foliar application has a stimulatory effect on phenylpropanoid and flavonoid pathways in grape berries. Frontiers in Plant Science **7**, 1150.

Conde C, Silva P, Fontes N, Dias ACP, Tavares RM, Sousa MJ, Agasse A, Delrot S, Gerós H. 2007. Biochemical changes throughout grape berry development and fruit and wine quality. Food **1**, 1–22.

Coombe BG. 1995. Growth stages of the grapevine: Adoption of a system for identifying grapevine growth stages. Australian Journal of Grape and Wine Research **1**, 100–110.

Dethloff F, Erban A, Orf I, Alpers J, Fehrle I, Beine-Golovchuk O, Schmidt S, Schwachtje J, Kopka J. 2014. Profiling methods to identify cold-regulated primary metabolites using gas chromatography coupled to mass spectrometry. Methods in Molecular Biology **1166**, 171–197.

Dimopoulos N, Tindjau R, Wong DCJ, Matzat T, Haslam T, Song C, Gambetta GA, Kunst L, Castellarin SD. 2020. Drought stress modulates cuticular wax composition of the grape berry. Journal of Experimental Botany **71**, 3126–3141.

Eulgem T, Somssich IE. 2007. Networks of WRKY transcription factors in defense signaling. Current Opinion in Plant Biology **10**, 366–371.

Feechan A, Jermakow AM, Torregrosa L, Panstruga R, Dry IB. 2008. Identification of grapevine *MLO* gene candidates involved in susceptibility to powdery mildew. Functional Plant Biology **35**, 1255–1266.

Fekete C, Fung RWM, Szabó Z, Qiu W, Chang L, Schachtman DP, Kovács LG. 2009. Up-regulated transcripts in a compatible powdery mildew–grapevine interaction. Plant Physiology and Biochemistry **47**, 732–738.

Feys BJ, Wiermer M, Bhat RA, Moisan LJ, Medina-Escobar N, Neu C, Cabral A, Parker JE. 2005. *Arabidopsis* SENESCENCE-ASSOCIATED $GENE_{101}$ stabilizes and signals within an ENHANCED DISEASE SUSCEPTIBILITY1 complex in plant innate immunity. The Plant Cell **17**, 2601–2613.

Ficke A, Gadoury DM, Seem RC, Dry IB. 2003. Effects of ontogenic resistance upon establishment and growth of *Uncinula necator* on grape berries. Phytopathology **93**, 556–563.

Fortes AM, Agudelo-Romero P, Silva MS, *et al.* 2011. Transcript and metabolite analysis in Trincadeira cultivar reveals novel information regarding the dynamics of grape ripening. BMC Plant Biology **11**, 149.

Fortes AM, Teixeira RT, Agudelo-Romero P. 2015. Complex interplay of hormonal signals during grape berry ripening. Molecules **20**, 9326–9343.

Fotopoulos V, Gilbert MJ, Pittman JK, Marvier AC, Buchanan AJ, Sauer N, Hall JL, Williams LE. 2003. The monosaccharide transporter gene, *AtSTP4*, and the cell-wall invertase, *Atbetafruct1*, are induced in Arabidopsis during infection with the fungal biotroph *Erysiphe cichoracearum*. Plant Physiology **132**, 821–829.

Fung RW, Gonzalo M, Fekete C, Kovacs LG, He Y, Marsh E, McIntyre LM, Schachtman DP, Qiu W. 2008. Powdery mildew induces defense-oriented reprogramming of the transcriptome in a susceptible but not in a resistant grapevine. Plant Physiology **146**, 236–249.

Gadoury DM, Cadle-Davidson L, Wilcox WF, Dry IB, Seem RC, Milgroom MG. 2012. Grapevine powdery mildew (*Erysiphe necator*): a fascinating system for the study of the biology, ecology and epidemiology of an obligate biotroph. Molecular Plant Pathology **13**, 1–16.

Gadoury DM, Seem RC, Ficke A, Wilcox WF. 2003. Ontogenic resistance to powdery mildew in grape berries. Phytopathology **93**, 547–555.

Gadoury DM, Seem RC, Pearson RC, Wilcox WF, Dunst RM. 2001. Effects of powdery mildew on vine growth, yield, and quality of Concord grapes. Plant Disease **85**, 137–140.

Gadoury DM, Seem RC, Wilcox WF, Henick-Kling T, Conterno L, Day A, Ficke A. 2007. Effects of diffuse colonization of grape berries by *Uncinula necator* on bunch rots, berry microflora, and juice and wine quality. Phytopathology **97**, 1356–1365.

Gao F, Dai R, Pike SM, Qiu W, Gassmann W. 2014. Functions of *EDS1-like* and *PAD4* genes in grapevine defenses against powdery mildew. Plant Molecular Biology **86**, 381–393.

Gao F, Shu X, Ali MB, Howard S, Li N, Winterhagen P, Qiu W, Gassmann W. 2010. A functional *EDS1* ortholog is differentially regulated in powdery mildew resistant and susceptible grapevines and complements an Arabidopsis *eds1* mutant. Planta **231**, 1037–1047.

Glazebrook J. 2005. Contrasting mechanisms of defense against biotrophic and necrotrophic pathogens. Annual Review of Phytopathology **43**, 205–227.

Gómez-Díaz E, Jordà M, Peinado MA, Rivero A. 2012. Epigenetics of host-pathogen interactions: the road ahead and the road behind. PLoS Pathogens **8**, e1003007.

Goyal N, Bhatia G, Sharma S, Garewal N, Upadhyay A, Upadhyay SK, Singh K. 2020. Genome-wide characterization revealed role of *NBS-LRR* genes during powdery mildew infection in *Vitis vinifera*. Genomics **112**, 312–322.

Griebel T, Zeier J. 2010. A role for β-sitosterol to stigmasterol conversion in plant-pathogen interactions. The Plant Journal **63**, 254–268.

Grimplet J, Pimentel D, Agudelo-Romero P, Martinez-Zapater JM, Fortes AM. 2017. The *lateral organ boundaries domain* gene family in grapevine: genome-wide characterization and expression analyses during developmental processes and stress responses. Scientific Reports **7**, 15968.

Grimplet J, Van Hemert J, Carbonell-Bejerano P, Díaz-Riquelme J, Dickerson J, Fennell A, Pezzotti M, Martínez-Zapater JM. 2012. Comparative analysis of grapevine whole-genome gene predictions, functional annotation, categorization and integration of the predicted gene sequences. BMC Research Notes **5**, 213.

Gu Z, Eils R, Schlesner M. 2016. Complex heatmaps reveal patterns and correlations in multidimensional genomic data. Bioinformatics **32**, 2847–2849.

Hayes MA, Feechan A, Dry IB. 2010. Involvement of abscisic acid in the coordinated regulation of a stress-inducible hexose transporter (VvHT5) and a cell wall invertase in grapevine in response to biotrophic fungal infection. Plant Physiology **153**, 211–221.

Heyer M, Reichelt M, Mithöfer A. 2018. A holistic approach to analyze systemic Jasmonate accumulation in individual leaves of *Arabidopsis* rosettes upon wounding. Frontiers in Plant Science **9**, 1569.

Hoffmann S, Di Gaspero G, Kovács L, Howard S, Kiss E, Galbács Z, Testolin R, Kozma P. 2008. Resistance to *Erysiphe necator* in the grapevine 'Kishmish vatkana' is controlled by a single locus through restriction of hyphal growth. Theoretical and Applied Genetics **116**, 427–438.

Hummel J, Strehmel N, Selbig J, Walther D, Kopka J. 2010. Decision tree supported substructure prediction of metabolites from GC-MS profiles. Metabolomics **6**, 322–333.

Jaillon O, Aury JM, Noel B, *et al.*; French-Italian Public Consortium for Grapevine Genome Characterization. 2007. The grapevine genome sequence suggests ancestral hexaploidization in major angiosperm phyla. Nature **449**, 463–467.

Jimenez-Aleman GH, Almeida-Trapp M, Fernández-Barbero G, Gimenez-Ibanez S, Reichelt M, Vadassery J, Mithöfer A, Caballero J, Boland W, Solano R. 2019. Omega hydroxylated JA-Ile is an endogenous bioactive jasmonate that signals through the canonical jasmonate signaling pathway. Biochimica et Biophysica Acta. Molecular and Cell Biology of Lipids **1864**, 158520.

Jones JD, Dangl JL. 2006. The plant immune system. Nature **444**, 323–329.

Jones L, Riaz S, Morales-Cruz A, Amrine KC, McGuire B, Gubler WD, Walker MA, Cantu D. 2014. Adaptive genomic structural variation in the grape powdery mildew pathogen, *Erysiphe necator*. BMC Genomics **15**, 1081.

Kim D, Langmead B, Salzberg SL. 2015. HISAT: a fast spliced aligner with low memory requirements. Nature Methods **12**, 357–360.

Kohorn BD, Kohorn SL. 2012. The cell wall-associated kinases, WAKs, as pectin receptors. Frontiers in Plant Science **3**, 88.

Koo AJ, Cooke TF, Howe GA. 2011. Cytochrome P450 CYP94B3 mediates catabolism and inactivation of the plant hormone jasmonoyl-L-isoleucine. Proceedings of the National Academy of Sciences, USA **108**, 9298–9303.

Koo AJ, Thireault C, Zemelis S, Poudel AN, Zhang T, Kitaoka N, Brandizzi F, Matsuura H, Howe GA. 2014. Endoplasmic reticulum-associated inactivation of the hormone jasmonoyl-L-isoleucine by multiple members of the cytochrome P450 94 family in *Arabidopsis*. The Journal of Biological Chemistry **289**, 29728–29738.

Kopka J, Schauer N, Krueger S, *et al.* 2005. GMD@CSB.DB: the Golm Metabolome Database. Bioinformatics **21**, 1635–1638.

Kusch S, Panstruga R. 2017. *mlo*-based resistance: an apparently universal "weapon" to defeat powdery mildew disease. Molecular Plant-Microbe Interactions **30**, 179–189.

Lara I, Belge B, Goulao LF. 2015. A focus on the biosynthesis and composition of cuticle in fruits. Journal of Agricultural and Food Chemistry **63**, 4005–4019.

Lara I, Heredia A, Domínguez E. 2019. Shelf life potential and the fruit cuticle: the unexpected player. Frontiers in Plant Science **10**, 770.

Lattanzio VMT, Cardinali A, Imperato F. 2006. Role of phenolics in the resistance mechanisms of plants against fungal pathogens and insects. Phytochemistry: Advances in Research **661**, 23–67.

Li H, Xu Y, Xiao Y, Zhu Z, Xie X, Zhao H, Wang Y. 2010. Expression and functional analysis of two genes encoding transcription factors, *VpWRKY1* and *VpWRKY2*, isolated from Chinese wild *Vitis pseudoreticulata.* Planta **232**, 1325–1337.

Liu X, Bai X, Wang X, Chu C. 2007. OsWRKY71, a rice transcription factor, is involved in rice defense response. Journal of Plant Physiology **164**, 969–979.

Lodhi MA, Ye G-N, Weeden NF, Reisch BI. 1994. A simple and efficient method for DNA extraction from grapevine cultivars and *Vitis* species. Plant Molecular Biology Reporter **12**, 6–13.

Luedemann A, Strassburg K, Erban A, Kopka J. 2008. TagFinder for the quantitative analysis of gas chromatography–mass spectrometry (GC-MS)-based metabolite profiling experiments. Bioinformatics **24**, 732–737.

Ma W, Guttman DS. 2008. Evolution of prokaryotic and eukaryotic virulence effectors. Current Opinion in Plant Biology **11**, 412–419.

Merz PR, Moser T, Höll J, Kortekamp A, Buchholz G, Zyprian E, Bogs J. 2015. The transcription factor VvWRKY33 is involved in the regulation of grapevine (*Vitis vinifera*) defense against the oomycete pathogen *Plasmopara viticola*. Physiologia Plantarum **153**, 365–380.

Nakamura Y, Mithöfer A, Kombrink E, Boland W, Hamamoto S, Uozumi N, Tohma K, Ueda M. 2011. 12-Hydroxyjasmonic acid glucoside is a COI1-JAZ-independent activator of leaf-closing movement in *Samanea saman*. Plant Physiology **155**, 1226–1236.

Ough CS, Berg HW. 1979. Powdery mildew sensory effect on wine. American Journal of Enology and Viticulture **30**, 321–321.

Özer N, Şabudak T, Özer C, Gindro K, Schnee S, Solak E. 2017. Investigations on the role of cuticular wax in resistance to powdery mildew in grapevine. Journal of General Plant Pathology **83**, 316–328.

Pap D, Riaz S, Dry IB, Jermakow A, Tenscher AC, Cantu D, Oláh R, Walker MA. 2016. Identification of two novel powdery mildew resistance loci, *Ren6* and *Ren7*, from the wild Chinese grape species *Vitis piasezkii*. BMC Plant Biology **16**, 170.

Pessina S, Lenzi L, Perazzolli M, Campa M, Dalla Costa L, Urso S, Valè G, Salamini F, Velasco R, Malnoy M. 2016. Knockdown of *MLO* genes reduces susceptibility to powdery mildew in grapevine. Horticulture Research **3**, 16016.

Petrovic T, Perera D, Cozzolino D, Kravchuk O, Zanker T, Bennett J, Scott ES. 2017. Feasibility of discriminating powdery mildew-affected grape berries at harvest using mid-infrared attenuated total reflection spectroscopy and fatty acid profiling. Australian Journal of Grape and Wine Research **23**, 415–425.

Piermattei B, Castellari M, Arfelli G. 1999. The phenolic composition of red grapes and wines as influenced by *Oidium tuckeri* development. Vitis **38**, 85–96.

Pike S, Gao F, Kim MJ, Kim SH, Schachtman DP, Gassmann W. 2014. Members of the NPF3 transporter subfamily encode pathogen-inducible nitrate/nitrite transporters in grapevine and Arabidopsis. Plant & Cell Physiology **55**, 162–170.

Qiu W, Feechan A, Dry I. 2015. Current understanding of grapevine defense mechanisms against the biotrophic fungus (*Erysiphe necator*), the causal agent of powdery mildew disease. Horticulture Research **2**, 15020.

Riaz S, Tenscher AC, Ramming DW, Walker MA. 2011. Using a limited mapping strategy to identify major QTLs for resistance to grapevine powdery mildew (*Erysiphe necator*) and their use in marker-assisted breeding. Theoretical and Applied Genetics **122**, 1059–1073.

Rietz S, Stamm A, Malonek S, Wagner S, Becker D, Medina-Escobar N, Corina Vlot A, Feys BJ, Niefind K, Parker JE. 2011. Different roles of Enhanced Disease Susceptibility1 (EDS1) bound to and dissociated from Phytoalexin Deficient4 (PAD4) in Arabidopsis immunity. New Phytologist **191**, 107–119.

Robert-Seilaniantz A, Grant M, Jones JD. 2011. Hormone crosstalk in plant disease and defense: more than just jasmonate-salicylate antagonism. Annual Review of Phytopathology **49**, 317–343.

Robinson MD, McCarthy DJ, Smyth GK. 2010. edgeR: a Bioconductor package for differential expression analysis of digital gene expression data. Bioinformatics **26**, 139–140.

Robinson MD, Oshlack A. 2010. A scaling normalization method for differential expression analysis of RNA-seq data. Genome Biology **11**, R25.

Rocha RO, Wilson RA. 2019. Essential, deadly, enigmatic: Polyamine metabolism and roles in fungal cells. Fungal Biology Reviews **33**, 47–57.

Roux M, Schwessinger B, Albrecht C, Chinchilla D, Jones A, Holton N, Malinovsky FG, Tör M, de Vries S, Zipfel C. 2011. The *Arabidopsis* leucine-rich repeat receptor-like kinases BAK1/SERK3 and BKK1/SERK4 are required for innate immunity to hemibiotrophic and biotrophic pathogens. The Plant Cell **23**, 2440–2455.

Rowland O, Ludwig AA, Merrick CJ, *et al.* 2005. Functional analysis of *Avr9/Cf-9 rapidly elicited* genes identifies a protein kinase, ACIK1, that is essential for full Cf-9-dependent disease resistance in tomato. The Plant Cell **17**, 295–310.

Schnee S, Viret O, Gindro K. 2008. Role of stilbenes in the resistance of grapevine to powdery mildew. Physiological and Molecular Plant Pathology **72**, 128–133.

Schulze B, Mentzel T, Jehle AK, Mueller K, Beeler S, Boller T, Felix G, Chinchilla D. 2010. Rapid heteromerization and phosphorylation of ligand-activated plant transmembrane receptors and their associated kinase BAK1. The Journal of Biological Chemistry **285**, 9444–9451.

Singleton VL, Rossi JA. 1965. Colorimetry of total phenolics with phosphomolybdic-phosphotungstic acid reagents. American Journal of Enology and Viticulture **16**, 144–158.

Soyer JL, Rouxel T, Fudal I. 2015. Chromatin-based control of effector gene expression in plant-associated fungi. Current Opinion in Plant Biology **26**, 51–56.

Staswick PE, Tiryaki I. 2004. The oxylipin signal jasmonic acid is activated by an enzyme that conjugates it to isoleucine in Arabidopsis. The Plant Cell **16**, 2117–2127.

Strehmel N, Hummel J, Erban A, Strassburg K, Kopka J. 2008. Retention index thresholds for compound matching in GC-MS metabolite profiling. Journal of Chromatography. B, Analytical Technologies in the Biomedical and Life Sciences **871**, 182–190.

Toth Z, Winterhagen P, Kalapos B, Su Y, Kovacs L, Kiss E. 2016. Expression of a grapevine NAC transcription factor gene is induced in response to powdery mildew colonization in salicylic acid-independent manner. Scientific Reports **6**, 30825.

Tsuda K, Mine A, Bethke G, Igarashi D, Botanga CJ, Tsuda Y, Glazebrook J, Sato M, Katagiri F. 2013. Dual regulation of gene expression mediated by extended MAPK activation and salicylic acid contributes to robust innate immunity in *Arabidopsis thaliana*. PLoS Genetics **9**, e1004015.

Vallarino JG, Erban A, Fehrle I, Fernie AR, Kopka J, Osorio S. 2018. Acquisition of volatile compounds by gas chromatography-mass spectrometry (GC-MS). Methods in Molecular Biology **1778**, 225–239.

Wagner S, Stuttmann J, Rietz S, Guerois R, Brunstein E, Bautor J, Niefind K, Parker JE. 2013. Structural basis for signaling by exclusive EDS1 heteromeric complexes with SAG101 or PAD4 in plant innate immunity. Cell Host & Microbe **14**, 619–630.

Wan J, Zhang XC, Neece D, Ramonell KM, Clough S, Kim SY, Stacey MG, Stacey G. 2008. A LysM receptor-like kinase plays a critical role in chitin signaling and fungal resistance in *Arabidopsis*. The Plant Cell **20**, 471–481.

Wang D, Pajerowska-Mukhtar K, Culler AH, Dong X. 2007. Salicylic acid inhibits pathogen growth in plants through repression of the auxin signaling pathway. Current Biology **17**, 1784–1790.

Wang S, Fu J. 2011. Insights into auxin signaling in plant–pathogen interactions. Frontiers in Plant Science **2**, 74.

Wang X, Guo R, Tu M, Wang D, Guo C, Wan R, Li Z, Wang X. 2017. Ectopic expression of the wild grape WRKY transcription factor VqWRKY52 in *Arabidopsis thaliana* enhances resistance to the biotrophic pathogen

powdery mildew but not to the necrotrophic pathogen *Botrytis cinerea*. Frontiers in Plant Science **8**, 97.

Wang Y, Liu Y, He P, Chen J, Lamikanra O, Lu J. 1995. Evaluation of foliar resistance to *Uncinula necator* in Chinese wild *Vitis* species. Vitis **34**, 159–164.

Weng K, Li ZQ, Liu RQ, Wang L, Wang YJ, Xu Y. 2014. Transcriptome of *Erysiphe necator*-infected *Vitis pseudoreticulata* leaves provides insight into grapevine resistance to powdery mildew. Horticulture Research **1**, 14049.

Zheng Z, Qamar SA, Chen Z, Mengiste T. 2006. Arabidopsis WRKY33 transcription factor is required for resistance to necrotrophic fungal pathogens. The Plant Journal **48**, 592–605.

Zhu Z, Shi J, Cao J, He M, Wang Y. 2012. *VpWRKY3*, a biotic and abiotic stress-related transcription factor from the Chinese wild *Vitis pseudoreticulata*. Plant Cell Reports **31**, 2109–2120.

Ziv C, Zhao Z, Gao YG, Xia Y. 2018. Multifunctional roles of plant cuticle during plant-pathogen interactions. Frontiers in Plant Science **9**, 1088.